UNITED NATIONS UNIVERSITY
GEOTHERMAL TRAINING PROGRAMME
Orkustofnun, Grensásvegur 9,
IS-108 Reykjavík, Iceland

Reports 2009
Number 6

GEOTHERMAL RESOURCE ASSESSMENT OF THE NW-SABALAN FIELD, IRAN, THROUGH WELL TESTING

Farhad Abdollahzadeh Bina
SUNA – Renewable Energy Organization of Iran
Yadegare Imam Highway, Poonake Bakhtari Ave.
Shahrake Ghods, P.O. Box 14155-6398
Tehran
IRAN
Abdollahzadeh_bina@yahoo.com

ABSTRACT

The assessment of the properties and capacity of geothermal resources involves various kinds of logging tests, data interpretation, monitoring and modelling. This ranges from the analysis of data collected during the warm-up and testing of single wells to the simulation of the response of the geothermal reservoir to utilization over years or even decades. This work presents a comprehensive review of the theoretical background and methodology used in analysing well-test, temperature- and pressure logging data from the Sabalan geothermal wells as well as a review of the methods generally used for geothermal reservoir pressure response modelling. These methods are then applied to data from the Sabalan geothermal field in northwest Iran. The purpose of the well test analysis is to identify the type of reservoir involved and to determine the parameters of the reservoir quantitatively. Data from three Sabalan wells, NWS-5D, NWS-6D and NWS-7D, was analyzed by the application of the computer software Well Tester developed by ÍSOR - Iceland GeoSurvey. This incorporates modern well-test analysis techniques such as derivative analysis and computer software simulation. Lumped parameter models have been used extensively to simulate data on pressure changes in geothermal systems in Iceland. The lump fit model analysis of injection test data from well RN-23 in Reykjanes, Iceland was used to estimate the permeability of the Sabalan field, and those results were then compared with the results from the Well Tester analysis. The volumetric method using the Monte Carlo simulation was applied to estimate the geothermal power potential of the Sabalan geothermal field given three scenarios of 25, 50 and 100 years duration.

1. INTRODUCTION

Iran covers 1,648,000 km^2 in southwest Asia. It is bordered by Azerbaijan, Armenia, Turkmenistan, and the Caspian Sea in the north, by Pakistan and Afghanistan in the east, by the Persian Gulf and the Gulf of Oman in the south, and by Turkey and Iraq in the west. Iran also controls about a dozen islands in the Persian Gulf. More than 30% of its 7,680 km (4,770 mile) border is coastline. Tehran is the capital. One of the most ancient cities in Iran is Meshkin Shahr, which is close to Mt. Sabalan. It is located in northwest Iran in the Azerbaijan part of Iran, some 839 km from Tehran and 160 km east of Tabriz (one of the large industrial cities). Tabriz is the closest large city to the Sabalan high mountain.

Mt. Sabalan is a large andesitic strato-volcano, the second highest volcano in Iran after Mount Damavand. The volcano is quite old, and its rocks have been dated back 5.6–1.4 million years. Some references, however, state that volcanic activity may have continued into the Holocene period, which started about 10,000 years ago. The summit region has several peaks exceeding 4,500 m a.s.l., primarily along a NE-SW trending ridge. The highest point is 4,811 m a.s.l. and is located at the northeastern end of the ridge. The mountain is located in a region with continental climate with hot, dry summers and extremely cold, snowy winters. Precipitation falls primarily as snow in the late autumn, winter and spring, and is sufficient to sustain seven glaciers near the summit above 4,000 m a.s.l. The largest of these was more than 1.5 km long during the 1970s. There are also extensive rock glaciers, several of which are more than 3 km in length. The Mt. Sabalan geothermal field is located in the Moil Valley on the northwest flank of Mt. Sabalan. The resource area has previously been identified by geoscientific studies as an approximately quadrangularly shaped area that covers approximately 75 km^2. SUNA – the Renewable Energy Organization of Iran has identified a potentially viable geothermal resource at Mt Sabalan.

2. THE SABALAN GEOTHERMAL FIELD

2.1 Geology

Mt. Sabalan lies on the South Caspian plate, which is under-thrust by the Eurasian plate to the north. It, in turn, is under-thrust by the Iranian plate, which produces compression in a northwest direction. This is complicated by a dextral rotational movement caused by a northward under-thrusting of the nearby Arabian plate beneath the Iranian plate. There is no Wadati-Benioff zone to indicate any present day subduction. The current project area is located within the Moil Valley which, on satellite and aerial photographic imagery, can be seen to be a major structural zone. Exposed on the valley surface are altered Pliocene volcanic activities, an unaltered Pleistocene trachydacite dome (Ar-Ar dated at 0.9 Ma) and Quaternary terrace deposits (Bogie et al., 2000). These units have been divided into four major stratigraphic units which, in order of increasing age, are (SKM, 2005):

- Quaternary alluvium, fan and terrace deposits;
- Pleistocene post-caldera trachyandesitic flows, domes and lahars;
- Pleistocene syn-caldera trachydacitic to trachyandesitic domes, flows and lahars;
- Pliocene pre-caldera trachyandesitic lavas, tuffs and pyroclastics.

The schematic geological map (Figure 1) shows the volcanic formations from the Eocene to the Quaternary period.

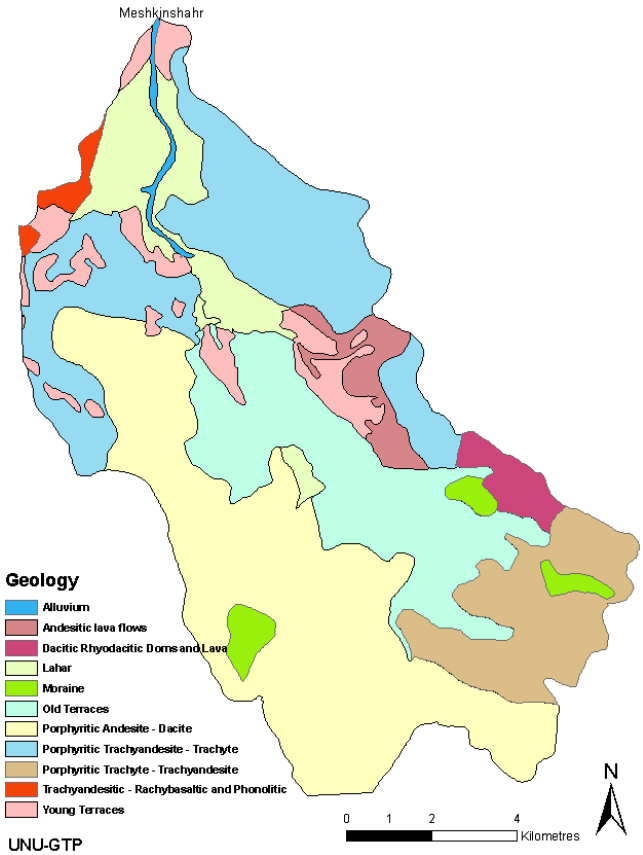

FIGURE 1: Geological map of the Sabalan–Meshkin Shahr prospect (modified from Yousefi-Sahzabi, 2004)

2.2 Geochemistry

Warm springs and hot springs with Cl-SO_4, and SO_4 chemistries are found within the valley (Bogie et al., 2000). The immature area of the Na-K-Mg plot gives geo-thermometry temperatures of approximately 150°C. One of these, the Gheynargeh (Qeynerce) spring has a Cl concentration of 1,800 mg/kg. Tritium analyses of this spring water indicate no recent interaction with the atmosphere. The isotopic composition of the spring waters and their seasonal variations in flow, and with little change in temperature or chemistry, suggest that a large regional groundwater aquifer overlies the main potential geothermal reservoir.

2.3 Geophysics

An MT survey (Bromley et al., 2000) established the existence of a very large zone (≈70 km^2) of low resistivity in the project area. Satellite image interpretation identified a large area (≈10 km^2) of hydrothermal alteration on the surface in the lower elevation parts of the project area, with much of the low resistivity area in the valley covered by Quaternary terrace deposits. The presence of hydrothermal alteration on the surface was confirmed by fieldwork. XRD analyses of this alteration reveals the presence of interlay red illite-smectite clays (which are conductive and will have formed at depth) indicating that at least some of the alteration and the resistivity anomaly is relict. At higher elevations unaltered rocks cover the zone of low resistivity. As a target area for drilling, an area of very low resistivity (< 4 Ωm) associated with the thermal features was initially selected. The early interpretation of the MT work (Bromley et al., 2000) shows low resistivity persisting to depth. However, once the relatively shallow occurrence of the conductive smectitic clays was established from the exploration geothermal wells, the MT data was reinterpreted in terms of the elevation of the base of the conductor. A conductive zone increasing in elevation to the south can be partially distinguished from the much larger and deeper resistivity anomaly to the west. This new interpretation is indicative of the current system's up-flow occurring south of the drilled wells (Talebi et al., 2005).

3. TEMPERATURE AND PRESSURE CONDITIONS IN THE SABALAN GEOTHERMAL FIELD

3.1 General information on the wells

On the basis of the results of the two MT surveys in 1997 and 2007, and the presence of hot springs with significant chloride concentrations, a three well exploration programme (NWS-1, NWS-3 and NWS-4) and three well delineation programme (NWS-5D, NWS-6D and NWS-7D) have been undertaken. The topography of the valley limits the location of drill pads to interconnected terraces, requiring five of the wells to be directionally drilled to access and extensively test the resistivity anomaly at depth. The drilling and testing programme for the exploration phase was carried out between November, 2002 and December, 2004, while the drilling and testing programme for the delineation phase was carried out between May, 2008 and August, 2009. The location of the project along with a detailed map of the drilled area is given in Figure 2. Of the six deep exploration and delineation wells that have been drilled, well NWS-1 was drilled from pad A, NWS-3 was drilled from pad C, NWS-4 and NWS-5D were drilled from pad B, and NWS-6D and NWS-7D were drilled from pad D. The wells vary in depth from 1,901 to 3,197 m MD. Well NWS-1 was drilled vertically while NWS-3, NWS-4, NWS-5D, NWS-6D and NWS-7D are deviated wells. Additionally, one shallow injection well, NWS-2, was drilled to 600 m depth, located on pad A alongside well NWS-1. The basic well completion data are summarised in Table 1.

TABLE 1: Basic completion information for the Sabalan wells

Well	Spud date	Completion date	Target depth mMD (mVD)	Production	Casing	Production	Liner
				Size (in)	Depth (mMD)	Size (in)	Depth (mMD)
NWS-1	22-Nov-02	01-Jun-03	3197	9-5/8	1586	7	3197
NWS-2	07-Jun-02	25-Jun-03	638	13-3/8	360	9-5/8, 5	638
NWS-3	02-Jul-03	27-Nov-03	3166 (2603)	13-3/8	1589	9-5/8	3160
NWS-4	17-Dec-03	27-Mar-04	2265.5 (1980)	9-5/8”	1166	7	2255
NWS-5D	30-May-08	31-Aug-08	1901	9-5/8”	750	7	1901
NWS-6D	16-Oct-08	28-Feb-09	2377	9-5/8”	1250	7	2377
NWS-7D	26-Mar-09	11-Aug-09	2705	9-5/8”	1313	7	2705

3.2 Well measurements

Here, the physical data from the wells is presented, including well completion information and downhole temperature and pressure data. The data has been used to define the sub-surface temperature and pressure distributions in the reservoir; the production potential of the wells; and the overall development potential of the resource.

3.2.1 Downhole well surveys

In Appendix I pressure and temperature profiles from the wells in the Sabalan field are presented. Figures 1-3 in the appendix showing the data for the exploration wells were taken from SKM reports (SKM, 2005), while Figures 4-6 show the data for the more recent delineation wells. The main results from Figures 4-6 are as follows:

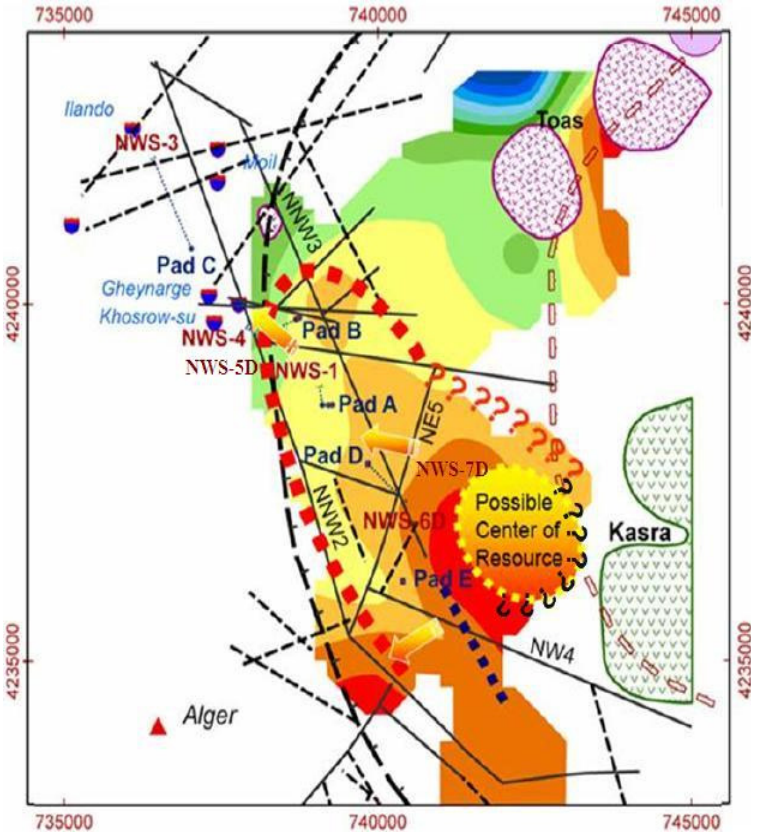

FIGURE 2: Well locations and the proposed geophysical model of the NW Sabalan geothermal system (EDC, 2009)

- The pivot points of wells NWS-5D and NWS-7D are at a pressure of about 120 bars;
- The pivot point for well NWS-6D is not clear;
- From the interpretations of all the pressure profiles it is concluded that, these wells are non-artesian, with no high pressure on the wellhead, and a water level that is deep in the wells. The wells must, therefore, be stimulated to flow.

The interpretations of the temperature profiles from the heating up, the injection test and during drilling are different.

- During heating, the feed zones from well NWS-6D can be seen as inversions in the temperature profile due to cooling from drilling.
- During injection, there can be seen a sudden increase in the temperature at the feed zones of well NWS 7D.

3.2.2 Interpretation of temperature logs

Determining the temperature distribution within a geothermal system is a fundamental requirement of any resource assessment study. The temperature distribution is probably the most useful information that can be obtained as it indicates both the quality of the resource and the fluid flow paths within the reservoir. To determine the sub-surface temperature distribution, it is first necessary to interpret the measured temperature surveys in the wells to establish the 'stable' reservoir conditions as a function of depth for each well, i.e. finding the rock temperature and the initial pressure of the reservoir. Contour plots and vertical cross-sections can then be prepared at selected depths and locations to show how the temperature varies within the reservoir, horizontally and vertically. These plots are useful for showing how hot and cold fluids interact within the geothermal system and are, therefore, very important in the formulation of the hydro-geological model of the system. The stable temperature profiles for wells NWS-1, NWS-3, NWS-4, NWS-5D, NWS-6D and NWS-7D have been determined based on the interpretation of the survey data presented in the figures in Appendix I and the resultant profiles are shown in Figure 3. A representative 'Boiling-Point-for-Depth' (BPD) curve is also shown, based on a measured water level of 2,413 m a.s.l. in well NWS-6D. By plotting the well temperature profiles together in Figure 3, it is possible to make some observations regarding the nature of the geothermal resource based on changes in temperature with depth:

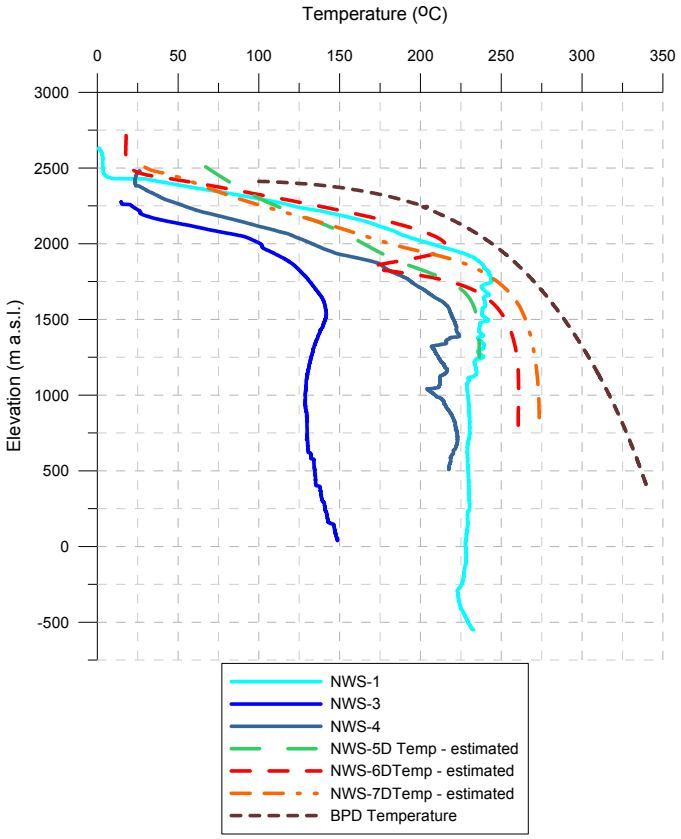

FIGURE 3: Stable well temperatures for the Sabalan wells

- The temperatures are all below the BPD curve, indicating that the reservoir in this area of the field does not contain a two-phase mixture of steam and water. Temperatures behind the casing of well NWS-1 at an elevation of about 1,900 m a.s.l. are close to BPD conditions, indicating a possible proximity to a two-phase fluid.
- Temperatures below the elevation of +1,500 m a.s.l. for wells NWS-5D, NWS-6D and NWS-7D are close to the BPD curve.
- From +1,500 m a.s.l. to between +600 and –200 m a.s.l. a slight temperature inversion is evident.
- Below -200 m a.s.l. in well NWS-1 and +600 m a.s.l. in well NWS-3, temperature increases with depth.
- The highest temperature has been estimated to be around 270–280°C in well NWS-7D, at an elevation of about +1,000 m a.s.l.
- Well NWS-1 is located closest to a deep upflow zone located in a generally southern direction.

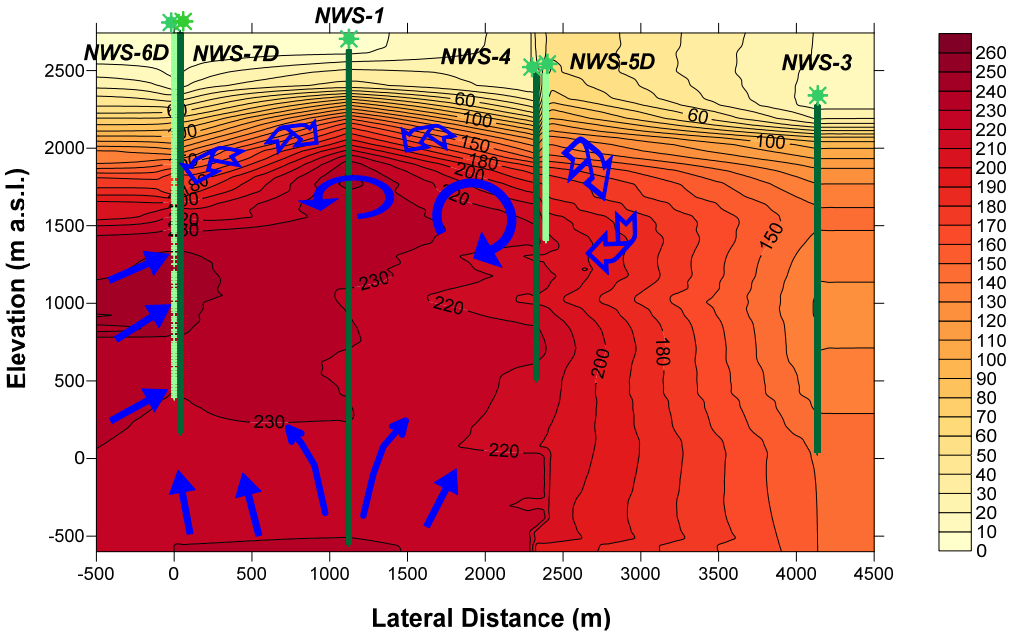

FIGURE 4: The Sabalan geothermal field temperature cross-section

The estimated stable temperatures derived from the available data from the six deep wells have been plotted on a temperature cross-section, which is shown in Figure 4. It is apparent from the temperature cross-section that there is hot outflow coming past well NWS-6D and flowing in the general direction of well NWS-3. Also, we can see the caprock thickness from an elevation of about 2,400 m a.s.l. to around 1,700 m a.s.l, so the main flow to the system is from the south and beneath the drilled area into the system. The system has a convective zone, at least 1.9 km thick, below approximately 1,500 m a.s.l. and caprock, around 700 m thick, with conductive heat flow.

3.2.3 Subsurface pressure distribution

Interpretation of sub-surface pressures is generally more difficult than sub-surface temperatures because the pressure profile within the wellbore does not generally reflect the pressure profile with depth in the surrounding formation. The wellbore pressure is often in equilibrium with the formation pressure only at the major feed zone. If there are two or more significant permeable zones then the depth of the equilibrium will lie between these zones. As the wellbore fluid heats up after drilling the hydrostatic gradient in the wellbore will change and the pressure profile measured in the well will pivot about the 'pressure control point' (PCP). The estimated pressure data has been used to construct a pressure cross-section, with the available data from the six deep wells. The cross-section is shown in Figure 5.

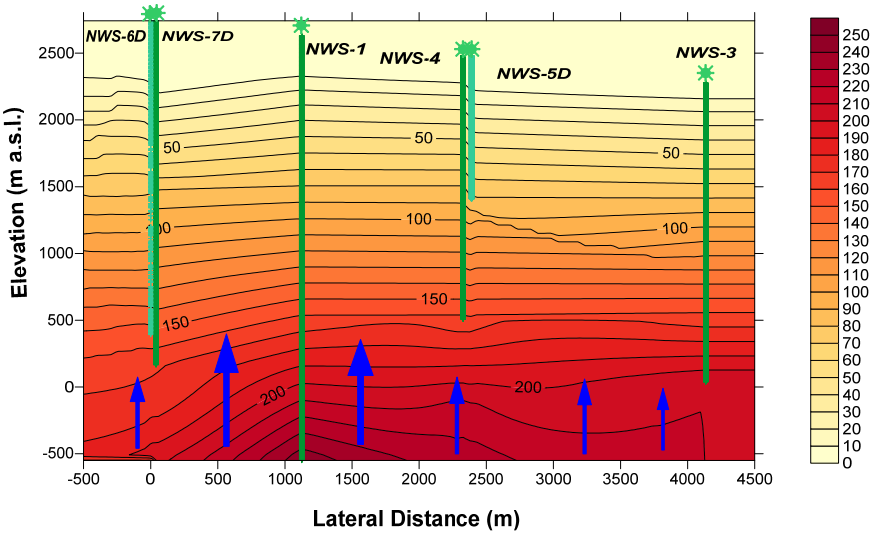

FIGURE 5: The Sabalan geothermal field pressure cross-section

4. THEORETICAL BACKGROUND ON WELL TESTING

4.1 Well and reservoir assessment procedures

In a hydrological well test, such as for a geothermal well, the pressure response of a given well and reservoir, due to production or injection, is monitored. Well testing is conducted in order to evaluate the conditions of a well, its flow capacity and the reservoir properties. The most important properties are the transmissivity or the permeability-thickness and the storativity or the formation storage coefficient of the reservoir. These are not evaluated directly from the data. The data has to be interpreted on the basis of the most appropriate model, resulting in average values. In addition, the properties are model dependent.

In Iran after a successful drilling programme, a typical high-enthalpy well assessment is undertaken through multi-step injection tests, in order to estimate the main physical properties of the reservoir around the well, like the transmissivity and storativity. This is done by assuming some values for the porosity and compressibility of the basaltic rock and fluid. Also, well parameters such as the injectivity index, the wellbore storage factor and the skin factor are determined in the step injection test. In this study a well test simulator program, Well Tester, was used to simulate data from such tests and then compare with the results from 'classic methods' like semi log, log-log and type curve methods. After this the well was closed in order to allow it to warm up and reach the steady-state formation temperature (often 3-4 months). During and after well testing, the temperature and pressure profiles of the well are logged and from that information the phase conditions of the fluid, the real formation temperature, the flow paths and the main feed zones can be obtained. However, caution must be taken when interpreting logs, as measurements are not made directly in the reservoir but in the well where internal flows and boiling can cause disturbances and give misleading results, even though the well is shut-in. When a well is not flowing, the aquifers (feed zones) usually warm up more slowly after drilling than impermeable rock, making it easier to determine the feed zones (Stefánsson and Steingrímsson, 1990).

4.1.1 The pressure diffusion equation

The basic equation in well testing theory is the pressure diffusion equation. It is used to calculate the pressure (P) in the reservoir at a certain distance (r) from a production well producing at a given rate (q) as a function of time (t). The most commonly used solution of the pressure diffusion equation is the so-called Theis solution or the line source solution. The three governing laws that are used in deriving the pressure diffusion equation are the following (Earlougher, 1977; Horne, 1995):

Conservation of mass inside a given control volume:

$$\textit{Mass flow in} - \textit{Mass flow out} = \textit{Rate of change of mass within the control volume}$$

Conservation of momentum, expressed by Darcy's law:

$$q = 2\pi r h \frac{k}{\mu}\frac{\partial P}{\partial r} \tag{1}$$

where q = Volumetric flow rate (m^3/s), q>0 for flow towards the well;
h = Reservoir thickness (m);
k = Formation permeability (m^2);
P = Reservoir pressure (Pa);
r = Radial distance (m);
μ = Dynamic viscosity of the fluid (Pa s).

The state of the fluid equation:

$$\rho = \rho(P, T) \tag{2}$$

The compressibility of the fluid equation:

$$c_f = \frac{1}{\rho}\left(\frac{\partial \rho}{\partial P}\right)_T \tag{3}$$

where c_f = Compressibility of the fluid (Pa^{-1});
ρ = Density of the fluid (kg/m^3);
T = Temperature (°C);
P = Pressure (Pa).

Initially the following simplifying assumptions are used:

- The reservoir is infinitely large and confined;
- The flow is considered isothermal and horizontal;
- The reservoir is considered homogeneous and isotropic;
- The producing well penetrates the entire formation thickness;
- The formation is completely saturated with a single fluid.

By combining the three equations above and using the above assumptions, the pressure diffusion equation is given by:

$$\frac{1}{r}\frac{\partial}{\partial r}\left(\frac{r\partial P(r,t)}{\partial r}\right) = \frac{\mu c_t}{k}\frac{\partial P(r,t)}{\partial t} = \frac{S}{T}\frac{\partial P(r,t)}{\partial t} \tag{4}$$

where $c_t = \varphi c_f + (1-\varphi)\, c_r$ = Total compressibility of rock and water (Pa^{-1});
φ = Porosity;
$c_r = \frac{1}{1-\varphi}\frac{\partial \varphi}{\partial P}$ is the compressibility of the porous rock;
$S = c_t h$ is the storativity; and
$T = \frac{kh}{\mu}$, is the transmisivity.

In 1935, Theis proposed an integral solution for this equation with (Earlougher, 1977; Horne, 1995):

Initial condition:

$P(r, t) = Pi$ for $t = 0$ $r > 0$

Boundary conditions:

i. $P(r, t) = Pi$ for $r \to \infty$ and $t > 0$

ii. $q = 2\pi r h \frac{k}{\mu}\frac{\partial P}{\partial r}$ for $r \to 0$ and $t > 0$

The solution to the radial diffusion equation with these boundary and initial conditions is given by:

$$P(r,t) = P_i + \frac{q\mu}{4\pi kh} Ei\left(\frac{-\mu c_t r^2}{4kt}\right) \tag{5}$$

where $Ei(-x) = -\int_x^\infty \frac{e^{-u}}{u} du$ is the exponential integral function

If $t > 100\frac{\mu c_t r^2}{4k}$ the exponential integral function can be expanded by a convergent series and, thus, the Theis solution for a pumping well with skin gives the total pressure change as:

$$\Delta P_t = P_i - P(r,t) = -\frac{2.303q\mu}{4\pi hk}\left[\log\left(\frac{\mu c_t r^2}{4kt}\right) + \frac{0.5772 - 2s}{2.303}\right] \quad (6)$$

where *s* is the skin factor, but skin is an additional pressure change to the normal pressure change in the near vicinity of the well due to the drilling of the well. A negative skin factor indicates that the well is in good communication with the reservoir.

4.1.2 Semi-logarithmic well test analysis

A plot of the Theis solution for ΔP_t vs. log *t* gives a semi-log straight line with a slope m per log cycle. This gives the response for an infinite acting radial flow period of a well. This method is referred to as semi-log analysis (Earlougher, 1977; Horne, 1995).

$$m = \frac{2.303q\mu}{4\pi kh}\ (Pa\ /\ \log cycle) \quad (7)$$

The skin-factor is given by:

$$s = 1.151\left[\frac{\Delta P_t}{m} - \log\left(\frac{k}{\varphi\mu c_t r_w^2}\right) - \log(t) - 0.351\right] \quad (8)$$

"The semi-log analysis is based on the interpretation of the semi-log straight line response that represents the infinite acting radial flow behaviour of the well. However, an actual wellbore has finite volume, and it becomes necessary to determine the duration of the wellbore storage effect or the time at which the semi-log straight line begins. The wellbore storage effect can be identified by a unit slope relationship when the data is plotted on a log (ΔP_t) vs. log (t) graph. After about 1½ log cycle from the end of the unit slope line, the semi log straight line is expected to start." (Earlougher, 1977; Horne, 1995).

"As time proceeds, the response is characteristic of conditions further and further away from the wellbore. At very late time, the pressure response is affected by the influence of reservoir boundaries, but prior to those late times the pressure response does not "see" the reservoir boundaries, and the reservoir acts as if it were infinite in extent. This intermediate time response, between the early wellbore-dominated response and the late time boundary-dominated response, is known as the infinite acting period." (Earlougher, 1977; Horne, 1995).

4.1.3 Type curve methods

Well test analysis often makes use of dimensionless variables. The importance of dimensionless variables is that they simplify the reservoir models by embodying the reservoir parameters (such as *k*), thereby reducing the total number of unknowns. They have the additional advantage of providing model solutions that are independent of any particular unit system. It is an inherent assumption in the definition that permeability, viscosity, compressibility, porosity, and thickness are all constants. The following dimensionless parameters are defined as:

Dimensionless pressure change:

$$P_D = \frac{2\pi kh}{q\mu}\Delta P \quad (9)$$

Dimensionless time:

$$t_D = \frac{kt}{c_t\mu r_w^2} \quad (10)$$

Dimensionless radial distance from the active well:

$$r_D = {}^{r}/_{r_w} \tag{11}$$

Even though the reservoir parameters have already been estimated, there are several advantages in performing a type curve match. Whereas the semi log method and the unit slope log-log line used only portions of the data, a type curve match uses the entire data set. This helps ensure consistency over the whole range of time, and also provides a mechanism to make use of the transition data which lies between the individual response periods. In a log-log type curve, it is known that the P_D versus t_D curves (the reservoir model) will have exactly the same shape as the $\Delta P_t = P_i - P(r_w,t)$ versus t data (the measurements during the well test) (Earlougher, 1977; Horne, 1995).

Generally, the procedure for type curve analysis can be outlined as follows (Earlougher, 1977; Horne, 1995):

- The data is plotted as log ΔP_t vs. log t on the same scale as that of the type curve;
- The curves are then moved, one over the other, by keeping the vertical and the horizontal grid lines parallel, until the best match is found;
- The best match is chosen and the pressure and time values are read from fixed points on the graphs, ΔP_M and P_{DM} as well as t_M and t_{DM};
- For an infinite acting system, the transmissivity, T, is evaluated from:

$$T = \frac{kh}{\mu} = \frac{q}{2\pi}\left(\frac{P_D}{\Delta P_t}\right)_M \tag{12}$$

and the storativity, S is calculated as:

$$S = c_t h = \frac{kh}{\mu r_w^2}\left(\frac{t}{t_D}\right)_M = \frac{T}{{r_w}^2}\,(\frac{t}{t_D})_M \tag{13}$$

4.1.4 Injection tests

Injection testing is in principle a simple variant of discharge flow testing, with the flow reversed. Water is injected into a well and the flow rate recorded along with the changes in the downhole pressure or the depth to the water level. A quasi-stable flow versus pressure curve can be obtained, and transient behaviour measured at changes in flow rate.

Injection is a simple inverse of production if the fluid injected is of the same enthalpy (quality or temperature) as that produced. Generally, the fluid injected is water that is cooler than the reservoir temperature and thus has different viscosity and compressibility than the reservoir fluid (Grant et al., 1982). The non-isothermal injectivity index obtained from these tests depends on the mobility ratio of the cold region to the hot reservoir and the extent of the cold spot. Sigurdsson et al. (1983) proposed a method for estimating the apparent viscosity which accounts for these effects and relates the non-isothermal injectivity index to the isothermal injectivity index. The injectivity index (*II*) obtained from injection tests, is often used as a rough estimate of the connectivity of the well to the surrounding reservoir. Here it is given in units [(L/s)/bar] and is defined as the change in the injection flow rate divided by the change in the stabilized reservoir pressure:

$$II = \left|\frac{\Delta Q}{\Delta P}\right| \tag{14}$$

where $\Delta Q = Q_{end\ of\ step} - Q_{beginning\ of\ step}$; and
$\Delta P = P_{end\ of\ step} - P_{beginning\ of\ step}$.

In Well Tester, the pressure values used to calculate *II* are taken from the modelled response (not the actual data collected).

5. INJECTION TEST DATA AND ITS INTERPRETATION

Most of the text in this section is generated from the Well Tester report generator. Therefore, there are repetitions seen in the text for the steps discussed below (Júlíusson et al., 2007).

5.1 Sabalan well NWS-5D

A four-rate step injection test was conducted in well NWS-5D on August 31st, 2008 that lasted about 18 hours. The pressure gauge used to monitor the pressure changes in the well was installed at around 1,300 m depth. The four step injection rates were 24, 32, 16 and 0 L/s, respectively (Figure 6). Interpretation of the pressure response curves of the injection steps from well NWS-5D is very difficult. In this report the pressure response curve of step number 2 was used, since this is the only step that could be analysed.

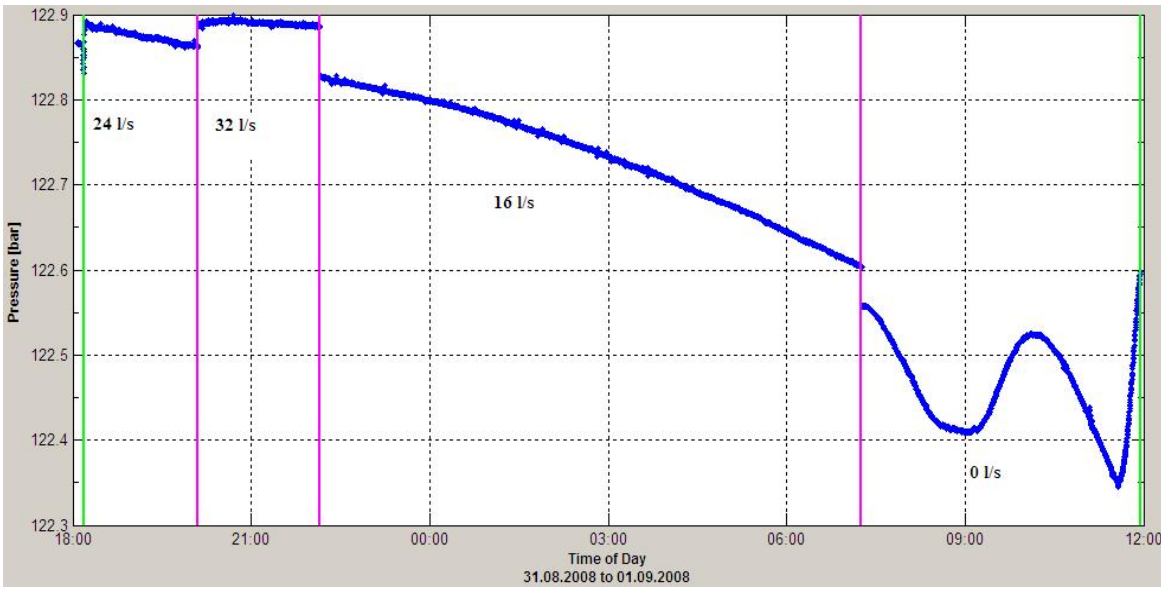

FIGURE 6: Pressures changes at 1,300 m depth in well NWS-5D during injection testing of the well on August 31st, 2008

5.1.1 Modelling step number 2

The well test model selected for step no. 2 is summarized in Table 2. Using this model, a non-linear regression analysis was performed to find the parameters that best fit the data gathered. The results from the regression analysis are shown graphically in Figure 7. Figure 8 shows additional plots of the same data on a log-linear scale (left) and log-log scale (right). The plot on the right also shows the derivative of the pressure response, multiplied by the time passed since the beginning of the step. This trend is commonly used to determine which type of model is most appropriate for the observed data. The parameters relevant to the selected model (Table 2) are shown in Table 3. The values shown for each parameter are the best estimate from the non-linear regression analysis. Moreover, the regression analysis gives information on the quality of the parameter estimates, represented here by the upper and lower limits of a 95% confidence interval and by the coefficient of variation C_v, given as a percentage in Table 3.

TABLE 2: Summary of the well testing model selected for step no. 2 in the injection test for NWS-5D

Part of system	Selected model
Reservoir	Dual porosity
Boundary	Constant pressure
Well	Constant skin
Wellbore	Wellbore storage

The values obtained for transmissivity and storativity can be used in conjunction with the given initial parameters to deduce an estimate on the reservoir thickness and the effective permeability. The estimated reservoir thickness is 1.90 km (1.90×10^3 m) and the effective permeability is 1.78×10^{-14} m^2 (≈ 17.8 mD). Note that these estimates rely on parameters that are generally quite poorly known and should, therefore, be viewed more as a qualitative order-of-magnitude check on the results of the well test.

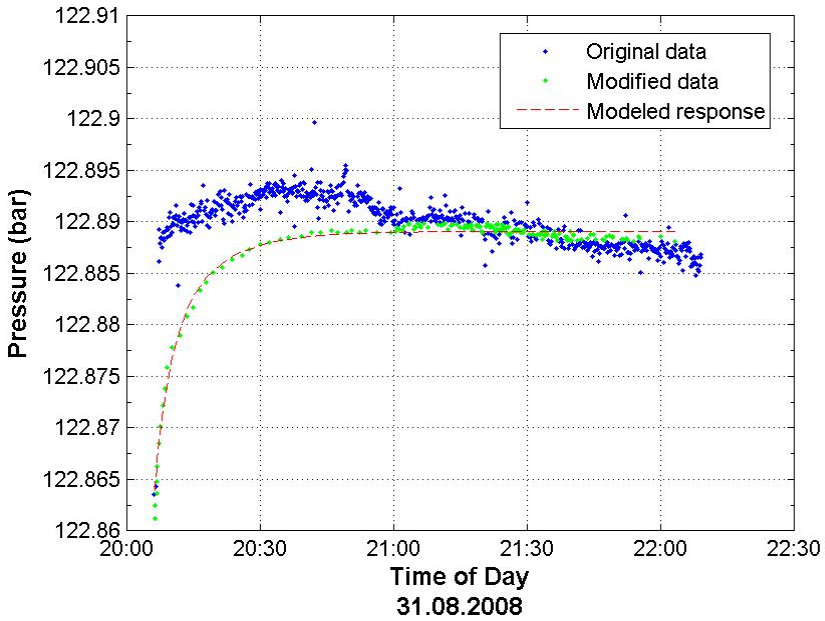

FIGURE 7: NWS-5D, fit between the well testing model and collected data for step no. 2

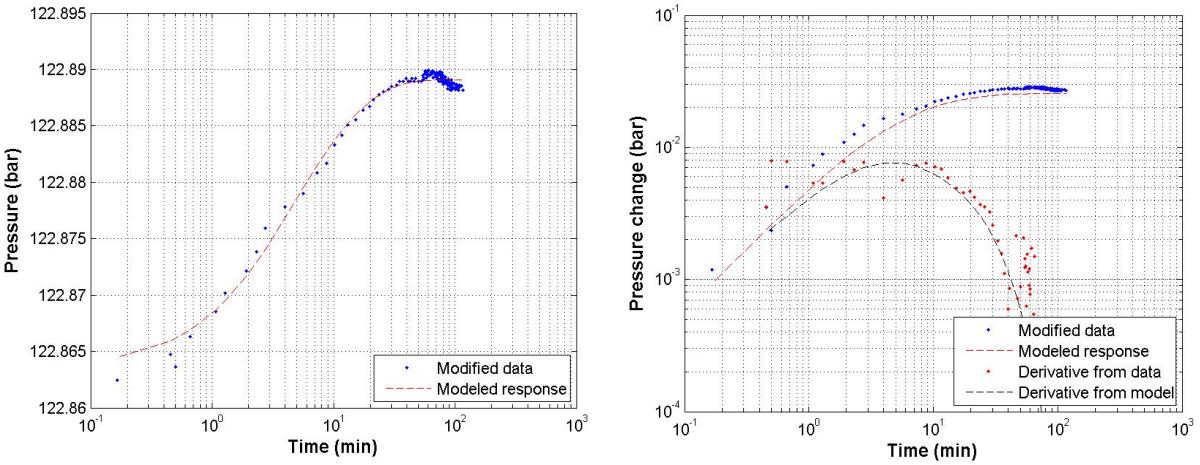

FIGURE 8: NWS-5D, fit between the well testing model and selected data on a log-linear scale (left) and a log-log scale (right); the derivative plot shown on the right is commonly used to determine the most appropriate type of model

TABLE 3: NWS-5D, summary of results from a non-linear regression parameter estimate for step no. 2

Parameter name	Parameter value	Lower bound 95 % C.I.	Upper bound 95 % C.I.	CV [%]	Parameter unit
Transmissivity (T)	2.76×10^{-6}	2.64×10^{-6}	2.88×10^{-6}	2.2	m^3/(Pa s)
Storativity (S)	1.02×10^{-7}	6.63×10^{-8}	1.38×10^{-7}	17.6	m^3/(Pa m^2)
Transmissivity ratio (λ)	1.00×10^{-10}	NaN	NaN	NaN	-
Storativity ratio (ω)	0.03	0.02	0.04	16.5	-
Radius of investigation (r_e)	1.79×10^3	1.35×10^3	2.23×10^3	12.3	m
Skin factor (s)	-3.73				-
Wellbore storage (C)	8.30×10^{-4}	7.68×10^{-4}	8.93×10^{-4}	3.8	m^3/Pa
Injectivity index (II)	314				(L/s)/bar

5.2 Sabalan well NWS-6D

A six-rate step injection test was conducted on March 29th, 2009 that lasted about 8 hours. The pressure gauge used to monitor the pressure changes in the well was installed at 1,485 m depth. The six step injection rates were 24, 30, 36, 40, 36 and 24 L/s, respectively (Figure 9). In this report the pressure response curves of steps no. 1 and 4 were used.

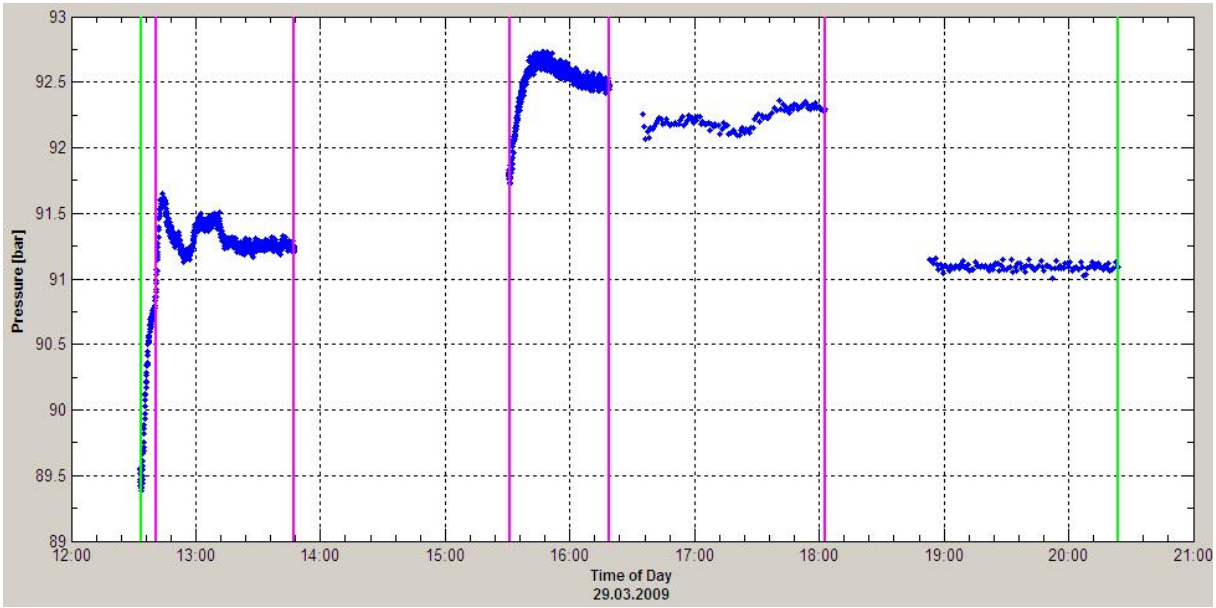

FIGURE 9: Pressure changes at 1,485 m depth in well NWS-6D during injection testing of the well on March 29th, 2009

5.2.1 Modelling step number 1

The well test model selected for step no. 1 is summarized in Table 4. Using this model, a non-linear regression analysis was performed to find the parameters that best fit the data gathered. The results from the regression analysis are shown graphically in Figure 10.

Figure 11 shows additional plots of the same data on a log-linear scale (left) and a log-log scale (right). The plot on the right also shows the derivative of the pressure response, multiplied by the time passed since the beginning of the step. The parameters

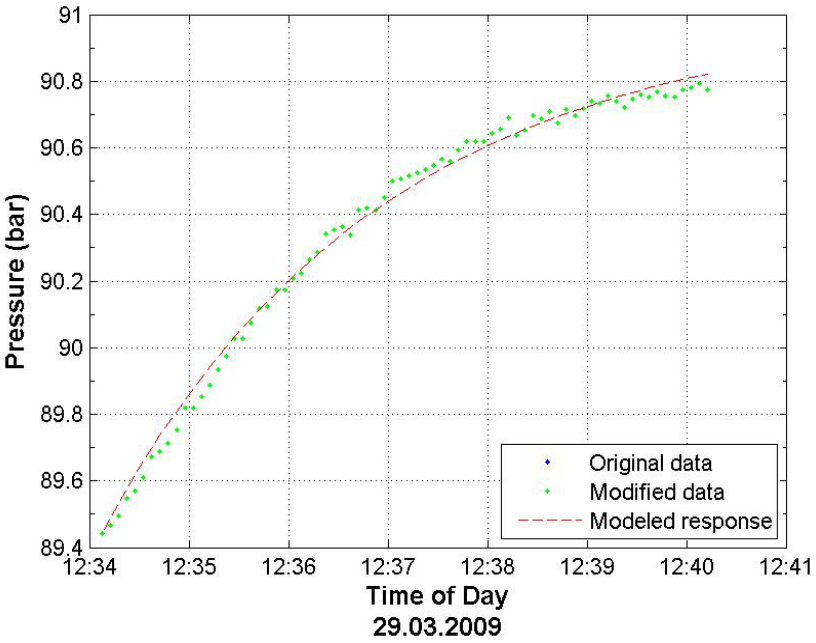

FIGURE 10: NWS-6D, fit between well testing the model and collected data for step no. 1

relevant to the selected model (Table 4) are shown in Table 5. The values shown for each parameter are the best estimate from the non-linear regression analysis.

TABLE 4: NWS-6D, summary of the well testing model selected for step no. 1

Part of system	Selected model
Reservoir	Dual porosity
Boundary	Infinite
Well	Constant skin
Wellbore	Wellbore storage

The values obtained for transmissivity and storativity can be used in conjunction with the given initial parameters to deduce an estimate on the reservoir thickness and the effective permeability. The estimated reservoir thickness is 1.82 km (1.82×10^3 m) and the effective permeability is 2.49×10^{-15} m^2 ($\approx$ 2.49 mD). Note that these estimates rely on parameters that are generally quite poorly known and should therefore be viewed more as a qualitative order-of-magnitude check on the results of the well test.

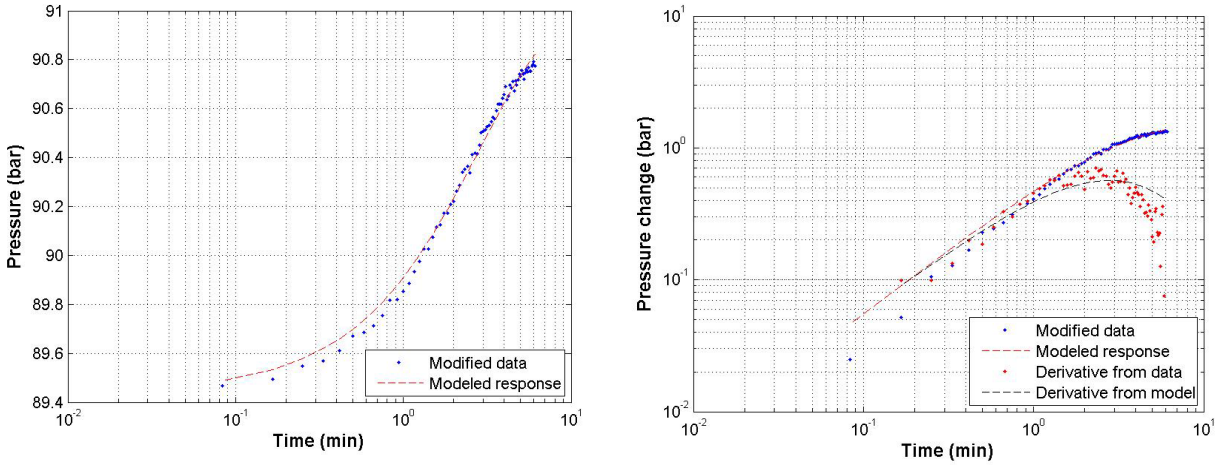

FIGURE 11: NWS-6D, fit between the model and selected data on a log-linear scale (left) and a log-log scale (right); the derivative shown on the right plot is commonly used to determine the most appropriate type of model

TABLE 5: NWS-6D, summary of the results from a non-linear regression parameter estimate for step no. 1

Parameter name	Parameter value	Lower bound 95 % C.I.	Upper bound 95 % C.I.	CV [%]	Parameter unit
Transmissivity (T)	3.85×10^{-8}	1.93×10^{-8}	5.76×10^{-8}	24.9	m^3/(Pa s)
Storativity (S)	1.01×10^{-7}	-1.57×10^{-7}	3.59×10^{-7}	127.1	m^3/(Pa m^2)
Transmissivity ratio (λ)	4.68×10^{-5}	-6.08×10^{-5}	1.54×10^{-4}	115.0	-
Storativity ratio (ω)	0.02	-0.02	0.05	114.0	-
Skin factor (s)	-0.45	-2.09	1.19		-
Wellbore storage (C)	8.49×10^{-6}	8.07×10^{-6}	8.92×10^{-6}	2.5	m^3/Pa
Injectivity index (II)	5.80				(L/s)/bar

5.2.2 Modelling step number 4

The well test model selected for step no. 4 is summarized in Table 6. Using this model, a non-linear regression analysis was performed to find the parameters that best fit the data gathered. The results from the regression analysis are shown graphically in Figure 12. Figure 13 shows additional plots of the same

TABLE 6: NWS-6D, summary of the well testing model selected for step no. 4

Part of system	Selected model
Reservoir	Dual porosity
Boundary	Infinite
Well	Constant skin
Wellbore	Wellbore storage

data on a log-linear scale (left) and a log-log scale (right). The plot on the right also shows the derivative of the pressure response, multiplied by the time passed since the beginning of the step.

The parameters relevant to the selected model (Table 6) are shown in Table 7. The estimated reservoir thickness is 1.82 km (1.82×10^3 m) and the effective permeability is 3.49×10^{-15} m^2 (≈ 3.49 mD).

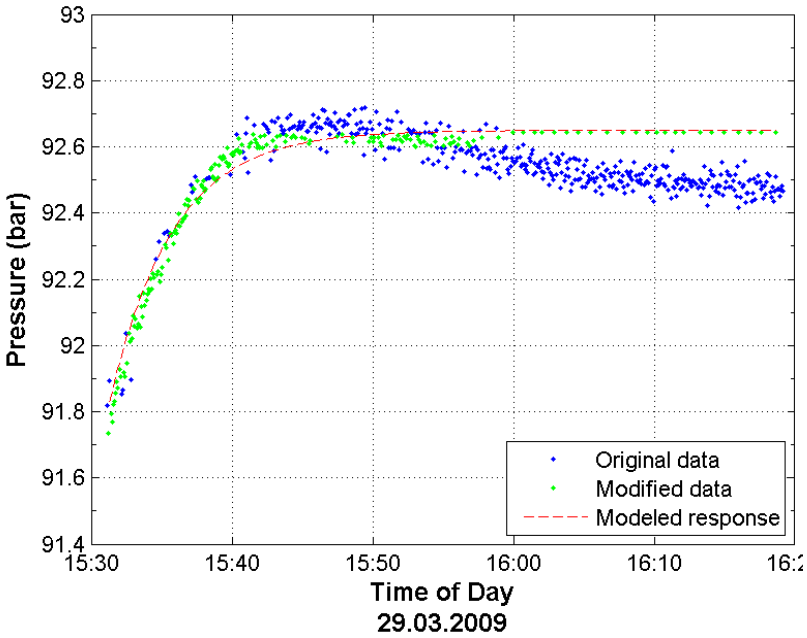

FIGURE 12: NWS-6D, fit between the model and collected data for step no. 4

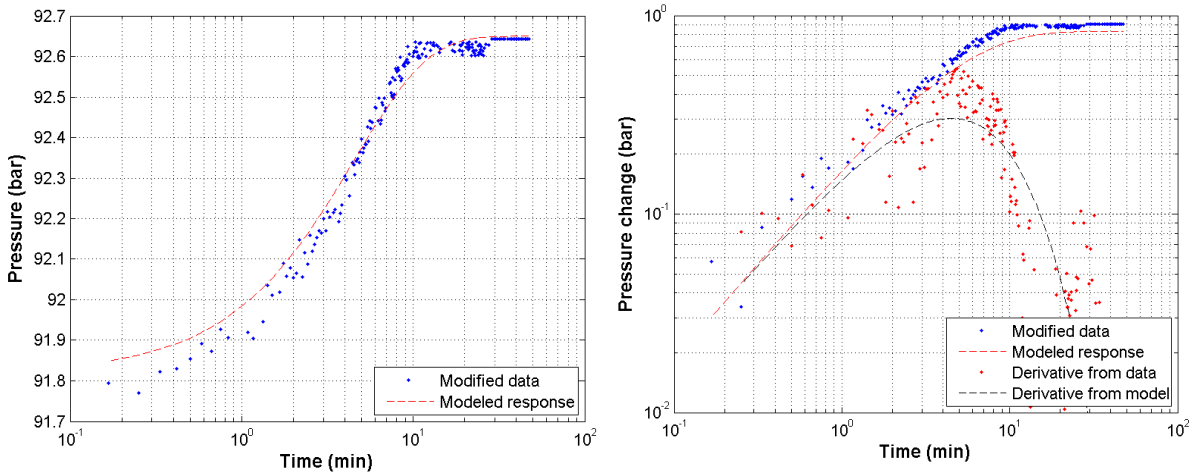

FIGURE 13: NWS-6D, fit between the model and selected data on a log-linear scale (left); and log-log scale (right).

TABLE 7: NWS-6D, summary of the results from a non-linear regression parameter estimate for step no. 4

Parameter name	Parameter value	Lower bound 95 % C.I.	Upper bound 95 % C.I.	CV [%]	Parameter unit
Transmissivity (T)	4.93×10^{-8}	2.92×10^{-8}	6.93×10^{-8}	20.4	m^3/(Pa s)
Storativity (S)	9.64×10^{-7}	-2.35×10^{-7}	2.16×10^{-6}	62.2	m^3/(Pa m^2)
Transmissivity ratio (λ)	3.11×10^{-6}	-8.72×10^{-6}	1.49×10^{-5}	190.0	-
Storativity ratio (ω)	2.00×10^{-4}	-9.97×10^{-4}	1.40×10^{-3}	299.4	-
Skin factor (s)	-0.66	-1.74	0.43		-
Wellbore storage (C)	1.01×10^{-5}	8.78×10^{-6}	1.14×10^{-5}	6.5	m^3/Pa
Injectivity index (II)	5.33				(L/s)/bar

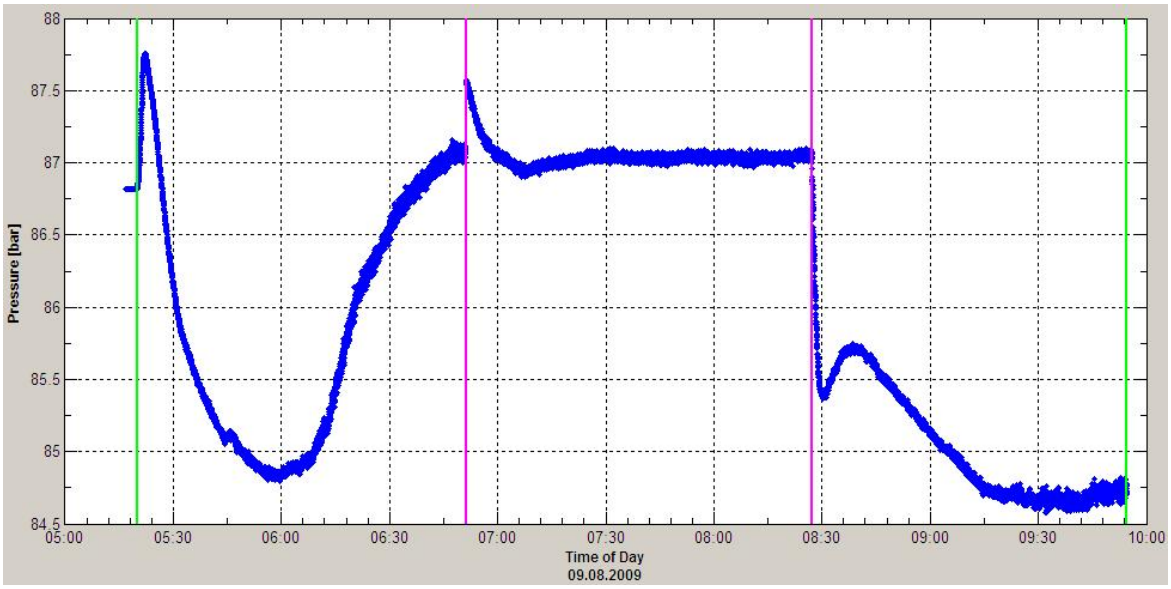

FIGURE 14: Pressure changes at 1,365 m depth in well NWS-7D during injection testing of the well on August 9th, 2009

5.3 Sabalan well NWS-7D

A three-rate step injection test was conducted on August 9th, 2009 that lasted about 4.5 hours. The pressure gauge used to monitor the pressure changes in the well was installed at 1,365 m depth. The three step injection rates were 24, 32 and 16 L/s, respectively (Figure 14). In this report, the pressure response curves of step number 3 were used.

TABLE 8: NWS-7D, summary of the well testing model selected for step no. 3

Part of system	Selected model
Reservoir	Dual porosity
Boundary	Infinite
Well	Constant skin
Wellbore	Wellbore storage

5.3.1 Modelling step number 3

The well test model selected for step no. 3 is summarized in Table 8. Using this model, a non-linear regression analysis was performed to find the parameters that best fit the data gathered. The results from the regression analysis are shown graphically in Figure 15. Figure 16 shows additional plots of the same data on a log-linear scale (left) and a log-log scale (right). The plot on the right also shows the derivative of the pressure response, multiplied by the time passed since the beginning of the step.

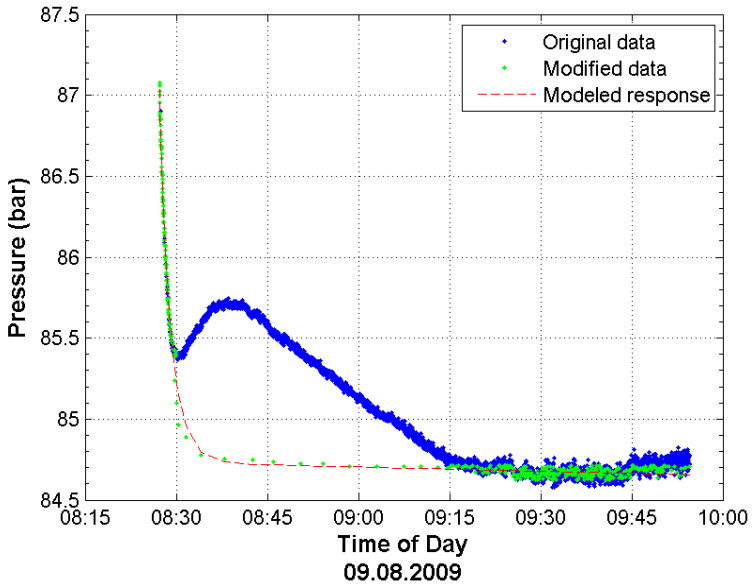

FIGURE 15: NWS-7D, fit between the well testing model and collected data for step no. 3

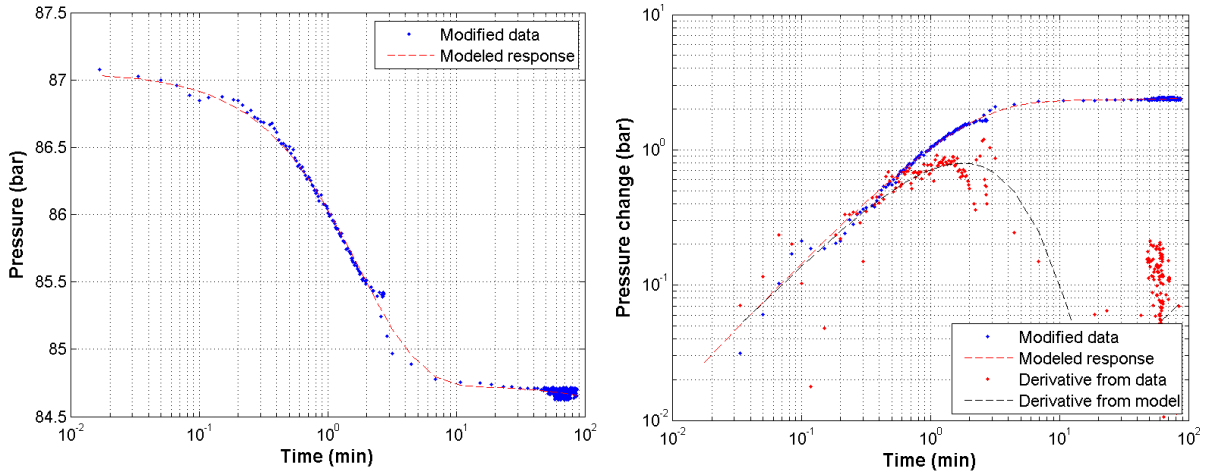

FIGURE 16: NWS-7D, fit between the model and selected data on a log-linear scale (left) and a log-log scale (right)

The parameters relevant to the selected model (Table 8) are shown in Table 9. The estimated reservoir thickness is 1.87 km and the effective permeability is 3.50×10^{-15} m^2 (≈ 3.50 mD).

TABLE 9: NWS-7D, summary of the results from a non-linear regression parameter estimate for step no. 3

Parameter name	Parameter value	Lower bound 95 % C.I.	Upper bound 95 % C.I.	CV [%]	Parameter unit
Transmissivity (T)	2.59×10^{-8}	2.40×10^{-8}	2.78×10^{-8}	3.6	m^3/(Pa s)
Storativity (S)	4.86×10^{-8}	4.38×10^{-8}	5.34×10^{-8}	4.9	m^3/(Pa m^2)
Transmissivity ratio (λ)	1.81×10^{-6}	1.33×10^{-6}	2.29×10^{-6}	13.3	-
Storativity ratio (ω)	3.83×10^{-3}	3.51×10^{-3}	4.15×10^{-3}	4.2	-
Skin factor (s)	-4.41	-4.54	-4.28		-
Wellbore storage (C)	6.06×10^{-6}	5.88×10^{-6}	6.25×10^{-6}	1.5	m^3/Pa
Injectivity index (II)	6.66				(L/s)/bar

5.4 Reykjanes well RN-23

5.4.1 General information on the Reykjanes geothermal field in Iceland

The Reykjanes geothermal field is one of several geothermal fields on the Reykjanes Peninsula, SW-Iceland, which covers the southwestern part of the western volcanic zone in Iceland. Initial development of the geothermal resources at Reykjanes dates back to around 1956, when the first exploratory well was drilled in the area. To evaluate the geothermal reservoir for the production of water and steam, extensive field investigations and drillings were carried out in the period between 1968 and 1970. This effort revealed a high-temperature geothermal resource. The reservoir temperatures are between 250 and 320°C, (Tómasson, 1971). The wells drilled produced high-pressure brine and steam. The development of the Reykjanes geothermal area was based on an interest in producing common salt from brine. A salt production plant was set up in the early 1970s along with a 0.5 MWe power plant. More recent resistivity studies (Karlsdóttir, 1997) delineate an area with an extent of ~ 10 km^2 for the Reykjanes geothermal system, whereas surface manifestations only cover about 1 km^2. Accelerated drilling was undertaken in Reykjanes during the period 2002 to 2009 and a total of 28 wells have been drilled for research and power production. A 100 MWe power plant was commissioned at Reykjanes in May 2006. The locations of wells drilled in the Reykjanes geothermal field are shown in Figure 17. Reykjanes was selected for comparison with Sabalan

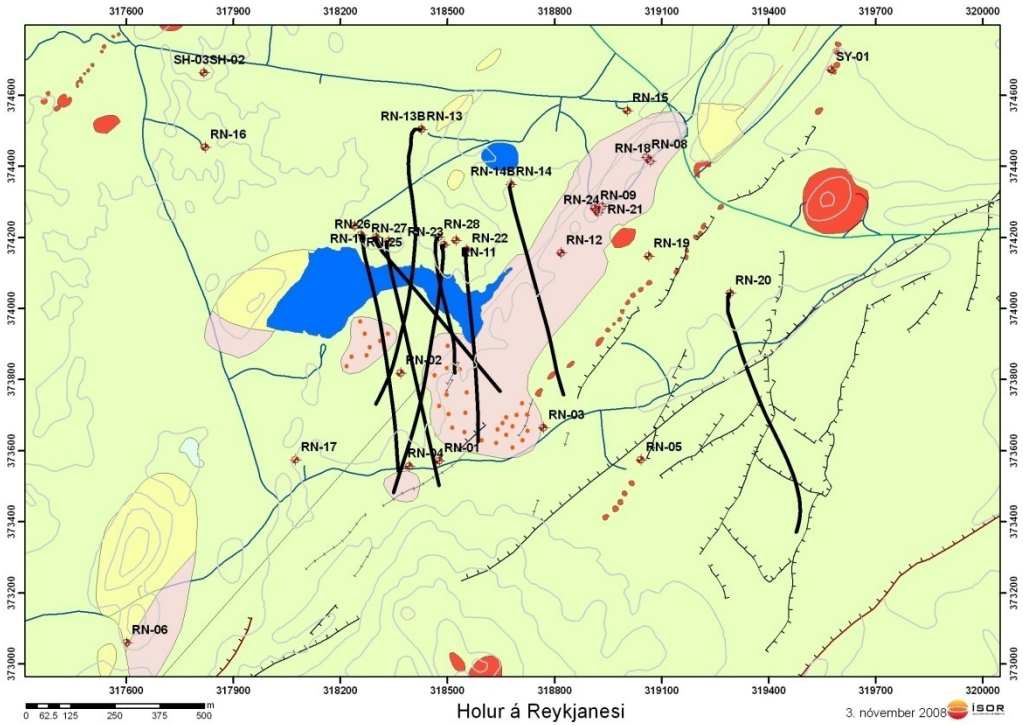

FIGURE 17: Geothermal manifestations and location of wells in the Reykjanes geothermal field

because injection tests in many wells in Reykjanes show very similar results, i.e. a high injectivity index and a small pressure change.

5.4.2 RN-23 Well Tester numerical software modelling

A three-rate step injection test was conducted in well RN-23 on March 21st, 2006 that lasted about 8 hours. The pressure gauge used to monitor the pressure changes in the well was installed at 1,330 m depth. The three step injection rates were 30, 45 and 60 L/s, respectively (Figure 18), with an initial injection of 65 L/s. In this report, the pressure response curves of steps number 2 and 3 were used. The well test model selected for modelling steps number 2 and 3 together is listed in Table 10.

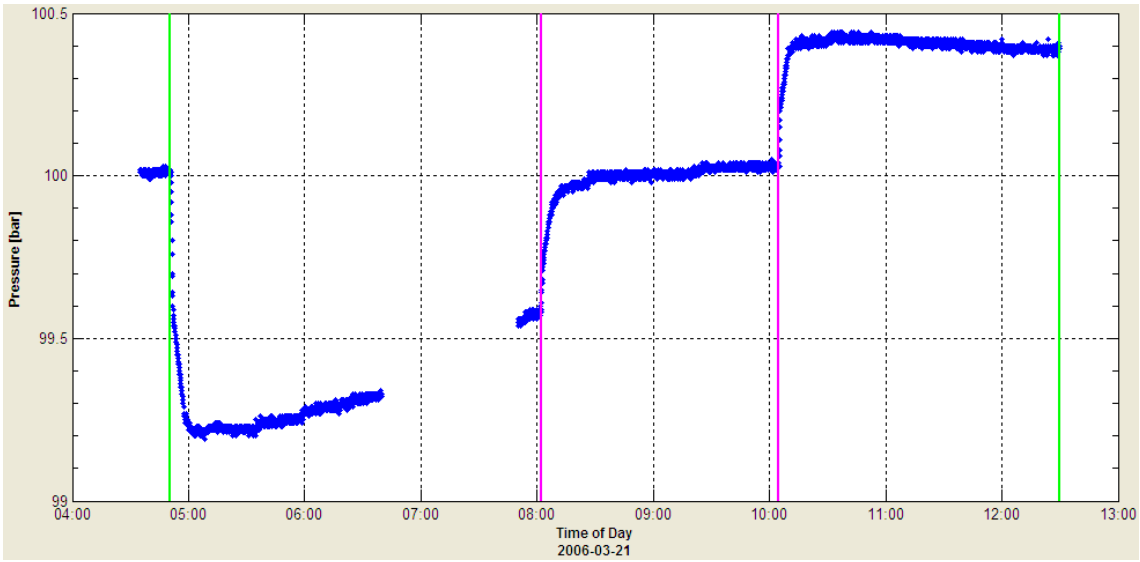

FIGURE 18: Pressure changes at 1,330 m depth in well RN-23 during injection testing of the well on March 21st, 2006

After numerical interpretation of the values from each step was done using this model, a non-linear regression analysis was used to find the parameters that best fit the observed data. The resulting fit is shown graphically in Figure 19.

TABLE 10: RN-23, summary of the well testing model selected for steps numbers 2 and 3 together

Part of system	Selected model
Reservoir	Dual porosity
Boundary	Infinite
Well	Constant skin
Wellbore	Wellbore storage

The parameters relevant to the selected model (Table 10) are shown in Table 11. The values shown for each parameter were the best estimate from the non-linear regression analysis. The estimated reservoir thickness is 1,810 m and the effective permeability is 1.60×10^{-14} m^2 ($\approx$ 16.0 mD). Note that these estimates rely on parameters that are generally quite poorly known and should therefore be viewed more as a qualitative order-of-magnitude check on the results of the well test.

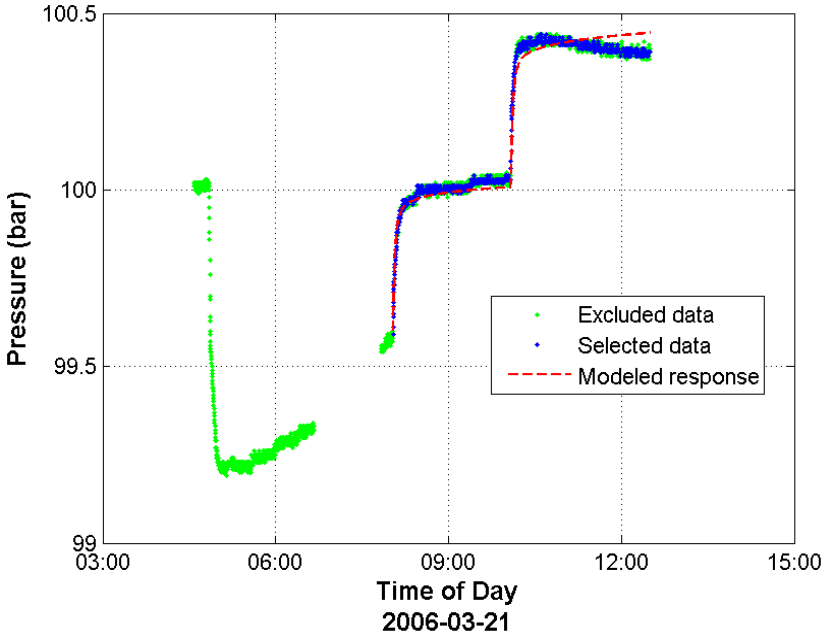

FIGURE 19: RN-23, fit between the well testing model and collected data for steps 2 and 3; parameters of the model are summarized in Table 11

TABLE 11: RN-23, summary of the results from a non-linear regression parameter estimate for steps 2 and 3

Parameter name	Parameter value	Lower bound 95 % C.I.	Upper bound 95 % C.I.	CV [%]	Parameter unit
Transmissivity (T)	3.34×10^{-7}	3.01×10^{-7}	3.68×10^{-7}	5.0	m^3/(Pa s)
Storativity (S)	5.92×10^{-7}	4.27×10^{-7}	7.58×10^{-7}	14.0	m^3/(Pa m^2)
Transmissivity Ratio (λ)	7.42×10^{-7}	2.21×10^{-7}	12.6×10^{-7}	35.1	-
Storativity Ratio (ω)	0.032	0.024	0.041	13.2	-
Skin Factor (s)	-1.43	-1.76	-1.11		-
Wellbore Storage (C)	3.08×10^{-5}	2.80×10^{-5}	3.36×10^{-5}	4.5	m^3/Pa
Injectivity Index (II)	36.8				(L/s)/bar

5.4.3 RN-23, lump-fit modelling

"Lumped parameter models have been used extensively to simulate data on pressure changes in geothermal systems in Iceland as well as in the P.R. of China, Central America, Eastern Europe, Philippines, Turkey and other countries. Lumped models can simulate such data very accurately, if

the data-quality is sufficient. The properties of the lumped models provide information on the corresponding properties of the geothermal system in question." (Axelsson et al., 2005). "Modelling plays an essential role in geothermal resource management and numerous examples are available on its successful application (Axelsson and Gunnlaugsson, 2000; O'Sullivan et al., 2001). This ranges from simple analytical modelling of the results of short well tests to detailed numerical modelling of complex geothermal systems, simulating an intricate pattern of changes resulting from long-term production. The purpose of geothermal modelling is, firstly, to obtain information on the physical conditions in a geothermal system as well as on its nature and properties. This leads to a proper understanding of its characteristics and the successful management of the resource. Secondly, the purpose of modelling is to predict the response of a reservoir to future production and estimate the production potential of a system, as well as to estimate the outcome of different management actions." (Axelsson et al., 2005).

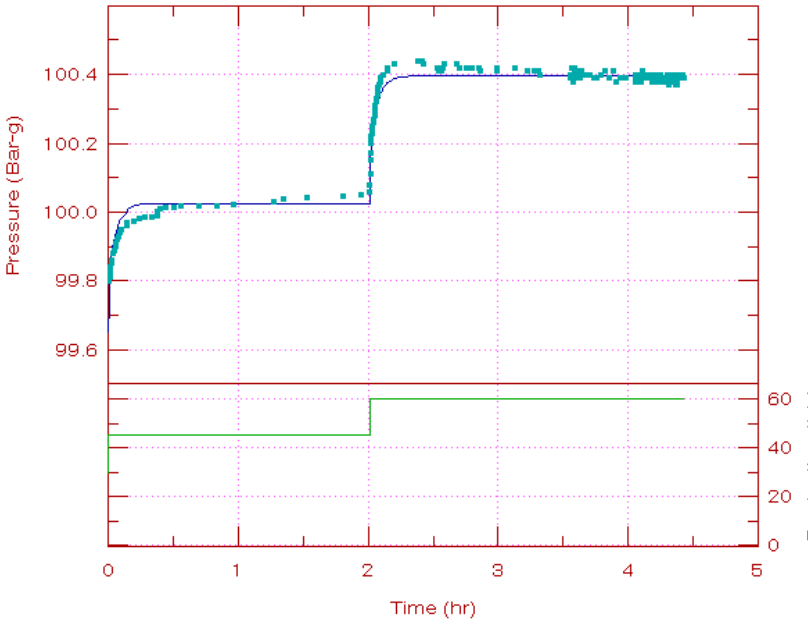

FIGURE 20: Injection and pressure change of well RN 23 in the Reykjanes geothermal field, March 21st, 2006

Figure 20 shows the pressure change simulation of well RN-23 that lasted about 5 hours on March 21st, 2006. It shows a very good agreement between the observed and simulated data. This reflects the efficiency and flexibility of the method of the lumped parameter modelling reviewed here. The reason for this is the diffusive nature of the pressure response of geothermal systems. The properties of the lumped models provide information on the corresponding properties of the geothermal system in question. The storage coefficients of the tanks (κ) provide information on the size of the geothermal system and on the controlling storage mechanism while the conductance (σ) of the resistors provides information on reservoir permeability. Furthermore, the model properties provide information on the boundary conditions that are in effect. The parameters of the lumped models are as follows:

One-tank closed model:

$$V = Ah \tag{15}$$

Storage mechanism:

$$\kappa = Ahs = Vs \tag{16}$$

Confined liquid-dominated reservoir:

$$s = \rho_w(\varphi c_w + (1-\varphi)c_r) \tag{17}$$

Unconfined (free – surface) reservoir:

$$s = \frac{\varphi}{gh} \tag{18}$$

Lump fit modelling gives κ_1, κ_2, κ_3. Make an assumption on the storage mechanism and porosity (φ) thus:

$$V_i = \frac{\kappa_i}{s} \tag{19}$$

The equations for a 2-D flow in a two-tank closed model are as follows:

$$k = \frac{\sigma_1 \ln ({}^{r_2}/_{r_1})\upsilon}{2\pi h} \tag{20}$$

$$R_1 = \sqrt{\frac{V_1}{\pi h}} \; and \; R_2 = \sqrt{(V_1 + V_2)/(\pi \cdot h)} \tag{21}$$

where $r_1 = \frac{R_1}{2}$;

$r_2 = R_1 + \frac{R_2 - R_1}{2} = \frac{R_1 + R_2}{2}$

V = Volume of the production part of the geothermal reservoir, or the mixing volume (m^3);
A = Surface area of the system (m^2);
h = Thickness of the reservoir (m);
k = Permeability of the aquitard (m^2);
ρ_w = Density of water (kg/m^3);
φ = Porosity of the reservoir (-);
c_w = Compressibility of water (Pa^{-1})
c_r = Compressibility of rock (Pa^{-1});
s = Storativity (s^2/m^2);
υ = Kinematic viscosity of water (m^2/s).

Also:

$$\sigma = \frac{q}{\Delta P} \quad and \quad \kappa = \frac{m}{p} \tag{22}$$

where q = Mass flow (kg/s);
ΔP= Pressure difference (Pa);
m = Mass increase (kg);
p = Pressure increase (Pa).

The parameters for the model that best fitted the data from the injection test of well RN-23 are listed in Table 12.

TABLE 12: The parameters of the lumped model for the injection test of well RN-23 (March 21st, 2006)

Number of tanks	Model type	A_1	A_2	κ_1	κ_2	σ_1	σ_2	Coefficient of determination
2	Open	64.69	7.08	0.13×10^{-1}	0.145	0.76×10^{-3}	0.77×10^{-3}	98.6%

By using these parameters, the main reservoir properties of the Reykjanes geothermal field could be estimated. Water compressibility c_w was estimated to be 3.5×10^{-9} Pa^{-1} at reservoir conditions (300°C). The compressibility of the rock matrix c_r, composed of basalt, is approximately 2×10^{-11} Pa^{-1}. The storativity of the Reykjanes reservoir was estimated using Equation 17 for the confined and Equation 18 for the unconfined reservoir. Then the value of the storativity can be used to estimate the reservoir volume and area by assuming a 2-D flow. The value $\varphi = 0.1$ was used for the porosity of the reservoir rock which is not fresh basalt. This value is commonly used in Iceland. Based on the well testing simulation of RN-23, a 1,000 m reservoir thickness was assumed, and considered for the calculations. Using the above series of equations, the principal properties and characteristics of the

reservoir, such as the volumes of different parts, their areas and permeability, could be deduced based on the 2-D flow model (see Table 13):

TABLE 13: Reservoir properties of the Reykjanes field according to lumped parameter models from well RN-23

Model	Properties		First tank	Second tank	Total
2-tank open	Reservoir volume (m^3)	Confined	57081	62367	6.8×10^5
		Unconfined	1304	14247	1.5×10^4
	Permeability (m^2)	Confined	-	-	1.7×10^{-14}
		Unconfined			6.6×10^{-16}

For the confined reservoir model, the permeability estimated is almost the same as the permeability estimated by the Well Tester, i.e. 16-17 mD.

6. VOLUMETRIC ASSESSMENT

6.1 Theory

An important factor in a geothermal assessment is the assessment of the volume of the geothermal system in question. For the volumetric method, we assume, for simplicity, that the volume is a box, with a surface area A in the *xy* plane and thickness z_1-z_0 along the z-axis, where z_1 and z_0 are the lower and upper limits of the geothermal system, respectively. The following discussion on theoretical aspects of columetric assessment is taken from Hjartarson et al., 2008).

"When the volume of the geothermal system has been assessed the choice has to be made on how to calculate the useable heat that the system contains. For simplicity it can be assumed that the heat capacity and temperature are homogeneous in the *xy* plane and are only dependent on depth. The heat content of the system can then be calculated by integrating the product of the estimated heat capacity per unit-volume *C(z)* and the difference between the estimated temperature curve *T(z)* in the system and the cut-off temperature T_0. The cut-off temperature is the temperature of the state from which the heat is integrated. This can be the outdoor temperature, minimum temperature for electric production, absolute zero temperature etc. The choice of *T(z)* depends on how one calculates the usable energy. We, therefore, get the heat energy contained in the geothermal system by:

$$Q = A \int_{z_0}^{z_1} C(z)[T(z) - T_0]\, dz \tag{23}$$

Only a small portion of the total heat in the system is recoverable; we define a recovery factor, *R*, the ratio of the heat which we can recover to the total heat in the system. The recoverable heat is therefore:

$$Q_R = RQ \tag{24}$$

The heat according to Equation 23 can be calculated in two ways. The first method is to integrate over the temperature curve and the second method is assuming that the temperature is also homogeneous in the *z* direction and therefore constant over the whole volume. This constant would be some mean temperature for the volume. The first method is appropriate if it is believed that the temperature curve is non-linear. But if it is believed that the temperature curve is close to being linear the second method would be more appropriate as the constant temperature would be the average temperature of the system. For simplicity the heat capacity per unit-volume will be taken as homogenous for the whole system and written as:

$$C = S_R(1 - \varphi)\rho_R + S_w \varphi \rho_w \tag{25}$$

where S_R and S_w are the specific heat of rock and water, respectively, ρ_R and ρ_w the density of rock and water, respectively, and φ is the porosity of the rock.

For the case of a non-linear temperature curve, which will be assumed from here on, it is convenient to assume that the temperature curve in the system follows a curve shaped like the boiling point curve (James, 1970):

$$T(z) = x.69.56(z + z_{Delta})^{0.2085} \tag{26}$$

Here x is a ratio factor running from zero to one describing the deviation from the true boiling curve, z_{Delta} is a translation in the z direction in order to fulfil the upper boundary conditions, T_{Z0} at z_0. Then we can write the recoverable heat described in Equation 24 as:

$$Q_R = RAC \int_{z_0}^{z_1} [T(z) - T_0]\, dz \tag{27}$$

From the recoverable heat of the geothermal system we can only utilise a small portion for electric production. We therefore define an electric utilization constant η_e which gives us the electric energy:

$$Q_e = \eta_e\, Q_R \tag{28}$$

and the electric power:

$$P = \frac{Q_e}{t} \tag{29}$$

where *t* is the production time of the electric power in seconds."

6.2 Monte Carlo calculations

"The variables used in the volumetric method are often shrouded with uncertainty and therefore it is necessary to define a probability distribution for these variables. By choosing one random value for each variable out of that probability distribution, one possible outcome of the volumetric method can be calculated. If this process is then repeated several times a discrete probability distribution for the outcome begins to form. This method of calculation is often named the Monte Carlo calculation after the Monte Carlo casino where a similar method is used for wealth distribution. To form the discrete distribution for the outcome we divide the interval of possible outcomes into equally long subintervals" (Hjartarson et al., 2008). The probability that the real outcome is in a particular subinterval is the ratio of possible outcomes that fall in that subinterval to the total number of possible outcomes that have been calculated. With the discrete probability distribution an opportunity emerges to evaluate the probability for the outcome to fall into a particular interval.

6.3 Evaluation of variables for the Sabalan field

To be able to perform the volumetric calculations we must estimate the value or probability distribution for the following variables:

1. Surface area of the geothermal system, *A*;
2. Thickness of the system, z_1-z_0;
3. Porosity of the rock, φ;
4. Mean physical characteristics of the rock and water in the system, that is the specific heat and density of the rock and water, S_R, S_w, ρ_R and ρ_w;
5. Heat distribution through the container, *T(z)*. This means the deviation ratio from the boiling curve, *x*, and the boundary condition z_{Delta};

6. Recovery factor, R;
7. Cut-off temperature, T_0.

These variables will give the heat that is recoverable from the system. To be able to evaluate the electric production capacity of the reservoir we also need values for the following variables:

8. Electric conversion coefficient, η_e;
9. Electric production time, t.

From the interpretation of the MT data and the surface geology we get the volume variables, the area A and lower depth z_1. The system is mainly made of par gneiss, so the range of values for porosity, rock density and the specific heat of the rock of the reservoir are chosen to be the same as for metamorphic rock (Freeze and Cherry, 1979). The recovery factor is a function of the porosity, as the heat is more difficult to extract from the rock with a lower porosity. Low values of porosity are expected for intrusive volcanic rock. For the upper layer the mean porosity used was 0.10 and the corresponding recovery factor used was 25%. For the deeper layers the mean porosity was 0.08 and the recovery factor used was 20% (Muffler, 1979).

In Figure 21 the temperature measurements in boreholes in the Sabalan area, along with some of the possible temperature curves $T(z)$ are shown. From this figure it is possible to draw a conclusion about the distribution of the boiling curve ratio, x, for our model. The boundary condition Z_{Delta} is calculated from the annual mean surface temperature which is taken to be 25°C. The cut-off temperature is chosen to be 180°C and the electric utilization constant is chosen accordingly (Wilcox, 2006). To estimate the possible electric power production we consider three production time scenarios, 25, 50 and 100 years. A summary of the parameters is given in Table 14.

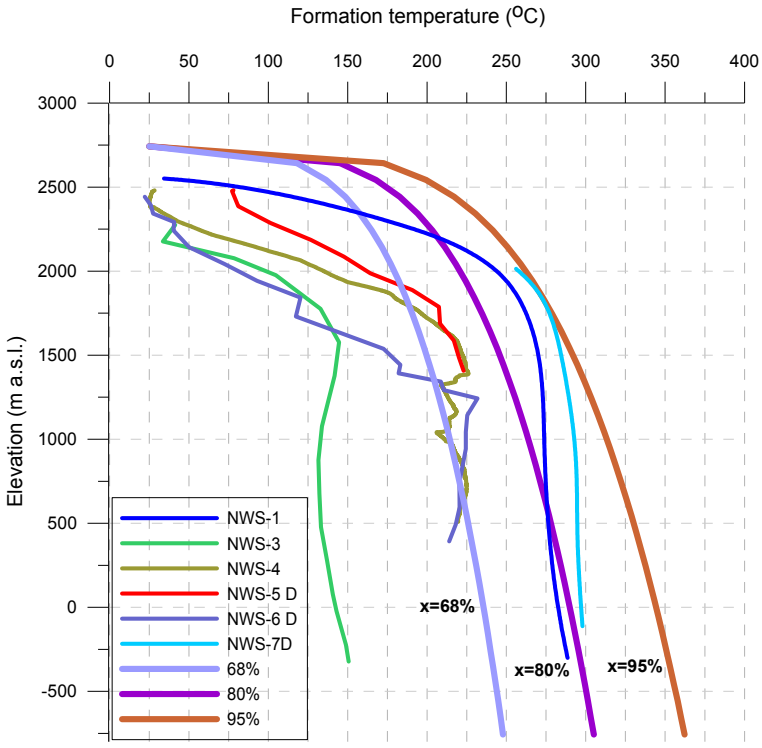

FIGURE 21: Formation temperature profiles measured and three possible temperature curves, based on the minimum, most likely and maximum values of the boiling curve ratio

6.4 Results of the volumetric calculations

An estimate of the electric power, which could be produced from the recoverable heat with a cut-off temperature of 180°C from the Sabalan geothermal reservoir, has been calculated according to Equation 29 above. This was done for three production time scenarios. The results are presented as a discrete probability distribution, seen in Figure 22, and as a discrete cumulative probability distribution, seen in Figure 23. Each figure consists of 100,000 random outcomes. From these random outcomes miscellaneous statistical information can be found. These include the likeliest outcome, 90% confidence interval, mean and median of the outcomes, standard deviation and where

TABLE 14: Values and distributions of the variables in the volumetric method

Description	Variable	Distribution type	Min. value	Most probable value	Max. value
Upper depth (m)	z_0	Fixed	N/A	0	N/A
Lower depth (m)	z_1	Triangular dist	2000	2500	3000
Surface area (km^2)	A	Triangular dist	10	19	30
Cut off temperature (^{o}C)	T_0	Fixed	N/A	180	N/A
Porosity (%)	φ	Triangular dist.	4	8	12
Specific heat of rock J/(kg ^{o}C)	S_R	Triangular dist	900	950	980
Density of rock (kg/m^3)	ρ_R	Fixed	N/A	2500	N/A
Specific heat of water J/(kg ^{o}C)	S_W	Fixed	N/A	4400	N/A
Density of water (kg/m^3)	ρ_W	Fixed	N/A	800	N/A
Boiling curve ratio (%)	x	Triangular dist	68	80	95
Recovery factor (%)	R	Triangular dist	15	20	25
Utilization constant (%)	η_e	Fixed	N/A	11	N/A
Production time (years)	t	Fixed	N/A	25, 50 or 100	N/A

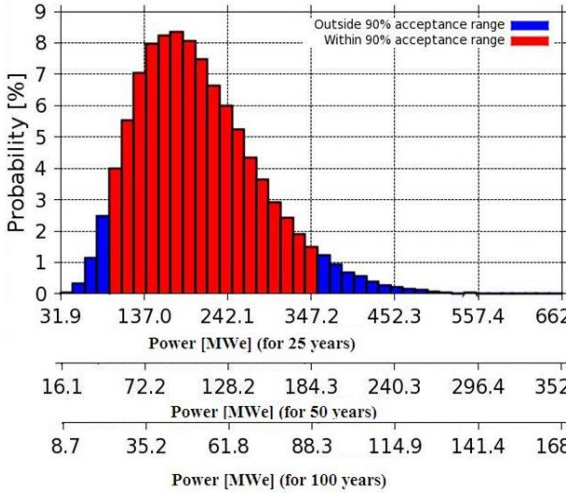

FIGURE 22: Probability distribution for electric power production; each pillar is about 16 MWe wide assuming 25 years, about 8 MWe for 50 years and about 4 MWe for 100 years. Statistical information for the distribution can be seen in Table 15

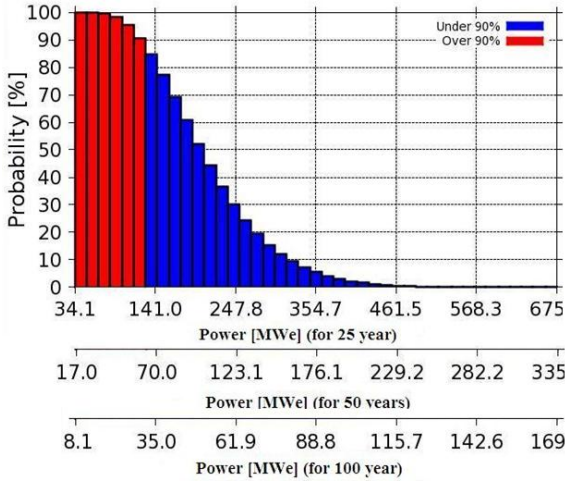

FIGURE 23: Cumulative probability distribution for electric power production; the pillars have the same width as given for Figure 22. The height of each pillar represents the probability that the result is in or above the interval of that pillar. In Table 15, the upper limit of the last pillar that is larger than 90% is presented

the 90% limit for the cumulative probability lies. These statistics are presented in Table 15 for each of the three production periods. According to the statistics of the probability distribution in Figure 22, it is most probable (with an 8.4% probability) that the electrical power production capacity lies between 170 and 186 MWe if the recoverable heat is used for 25 years, between 90 and 98 MWe if it is used for 50 years and between 44 and 47 MWe if it is used for 100 years. Also, from the statistics of the distribution in Figure 22, it is seen that the volumetric model predicts that with 90% confidence the power production lies between 93 and 355 MWe for 25 years, between 41 and 180 MWe for 50 years and between 24 and 90 MWe for 100 years.

It should be emphasized that the great range of values resulting from the Monte Carlo calculations simply reflects the uncertainty in the results obtained by the volumetric assessment method. It is

primarily caused by an uncertainty in the size, temperature and recovery factor for the Sabalan geothermal reservoir resource. If reinjection were to be applied during utilization to supplement natural recharge, a higher lower limit for the recovery factor could be used, raising the lower limit for the production capacity estimate.

TABLE 15: Statistical parameters for the probability distribution for electric power production from the Sabalan geothermal field estimated by the Monte Carlo method

Statistical size	Values (MWe) (for 25 years)	Values (MWe) (for 50 years)	Values (MWe) (for 100 years)
Most probable value (with 8.4% probability)	170 – 186	90 – 98	44 – 48
90% confidence interval	93 – 355	41 – 180	24 – 90
Mean value	206	103	52
Median value	195	98	49
Standard deviation	78	39	20
90% limit	128	64	32

7. CONCLUSIONS AND RECOMMENDATIONS

In summary, the main results of the analysis of data from wells NWS-5D, NWS-6D and NWS-7D are:

- The main flow to the system is from the south and beneath the drilled area into the system.
- The northwest part of the Sabalan geothermal system has at least around a 2 km thick convective zone below approximately 1,500 m a.s.l. and around 700 m thick caprock with a conductive heat flow.
- The estimated permeability for well NWS-5D is about 18 mD, skin factor is -3.7 and II is about 314 (L/s)/bar. The main feed zone of well NWS-5D is at around 1,100–1,300 m depth.
- The estimated permeability for well NWS-6D is about 3 mD, skin factor is -0.5 and II is about 5.5 (L/s)/bar. The main feed zone of well NWS-6D is at around 1,485 m depth.
- The estimated permeability for well NWS-7D is about 3.5 mD, skin factor is -4.5 and II is about 6.6 (L/s)/bar. The main feed zone of well NWS-7D is at around 1,365 m depth.
- The permeability of well RN-23 is most like that of well NWS-5D, but somewhat higher than the permeability for wells NWS-6D and NWS-7D; this can also be seen in the injectivity index which is higher for wells NWS-5D and RN-23 than for wells NWS-6D and NWS-7D.
- Results for the permeability from the Well Tester and lump fit model are of the same magnitude for well RN-23.
- A Monte Carlo volumetric capacity assessment, based on the available data, was performed. An estimate for the electric power, which can be produced from the recoverable heat in the geothermal region, was calculated. According to the statistics of the probability distribution the electrical power capacity will be, with 90% confidence, 93-355 MWe if the recoverable heat is used for 25 years. It will be in the range 41-180 MWe if it is used for 50 years and in the range 24-90 MWe if it is used for 100 years. The great range of these estimates simply reflects the uncertainty in the size, temperature and recovery factor for the Sabalan resource. For example if a lower limit for the recovery factor of 15% was used, and if reinjection were to be applied during utilization, a higher lower limit for the recovery factor could be used, raising the lower limit for the electrical power capacity estimate.

Some recommendations can be made to improve the data quality and consequent data interpretation such as:

- The reservoir response to production from the three new wells (NWE-5D, NWS-D and NWS-7D) should be monitored for an estimation of the productivity index (*PI*) and the calculation of the ratio between the injectivity index (*II*) and the productivity index (*PI*) for each well.
- Comparison between the new well at Sabalan and well RN-23 in Reykjanes, Iceland shows that there are similarities between the two reservoirs and thus it might be possible to use the experience from Reykjanes in the future development of the Sabalan geothermal reservoir.
- A new MT survey should be undertaken to better define the known field boundaries and to establish the field's southern and western extents.
- A new well should be drilled from pad E in a southerly direction.
- The data and information should be stored in a database system, for example Oracle.
- Numerical reservoir modelling (e.g. using TOUGH2) should be conducted after collecting data on long term production and logging of pressure and temperature.

After a successful program of geothermal well drilling, it is recommended that the following main steps be taken before those wells are connected to a power station, in order to get a good evaluation of the reservoir properties:

- Multi-step injection, interference and build-up tests.
- Data analysis with 'classic' (semi log, log-log, type curves) and 'modern' (derivative plots, well test simulator) methods.
- Close a well for 2-3 months before discharging in order for it to warm-up and reach a steady state formation temperature.
- Pressure and temperature profiles should be measured regularly for the whole time.
- Production tests should be performed after opening the wells.

ACKNOWLEDGEMENTS

I am thankful to God for protecting me and my family during my study in Iceland and enabling me to take this course and finish it. I would like to express my deepest gratitude to Dr. Ingvar B. Fridleifsson, Director, and Mr. Lúdvík S. Georgsson, Deputy Director, for giving me the opportunity to attend the UNU Geothermal Training Programme in 2009. I am grateful to my supervisors, Páll Jónsson, Hédinn Björnsson and Saeunn Halldórsdóttir for their continuous supervision and valuable discussions during my work and to Dr. Gudni Axelsson for valuable comments to improve the report. Furthermore, thanks go to Ms. Thórhildur Ísberg, Ms. Dorthe H. Holm and Mr. Markús A.G. Wilde for their help during the course. I would also like to give thanks to Mr. Armoodli, Managing Director of SUNA - the Renewable Energy Organization of IRAN, Mr. Ramezani, Deputy Managing Director of SUNA, Mr. Porkhial, the Sabalan Geothermal Project Director and Mr. Khosrawi, the Sabalan Geothermal Project Site Manager for supporting me during these 6 months. I am also grateful to the staff members of the Sabalan geothermal project, especially Mr. Behnam Radmehr for his technical support.

Last and definitely not least, I'm very grateful to my family, especially my wife, Parnaz Johari, for their support, prayers and encouragement throughout my stay in Iceland.

REFERENCES

Axelsson, G., Björnsson, G. and Quijano, J. E., 2005: Reliability of lumped parameter modelling of pressure changes in geothermal reservoirs. *Proceedings of the World Geothermal Congress 2005, Antalya, Turkey,* CD, 8 pp.

Axelsson, G., and Gunnlaugsson E. (convenors), 2000: *Long-term monitoring of high- and low-enthalpy fields under exploitation.*, World Geothermal Congress 2000, short course, Japan, 226 pp.

Bogie, I., Cartwright, A.J., Khosrawi, K., Talebi, B. and Sahabi, F., 2000: The Meshkin Shahr geothermal prospect, Iran. *Proceedings of the World Geothermal Congress 2000, Kyushu-Tohoku, Japan,* 997-1002.

Bromley, C., Khosrawi, K., and Talebi, B., 2000: Geophysical exploration of Sabalan geothermal prospect in Iran. *Proceedings of the World Geothermal Congress 2000, Kyushu-Tohoku, Japan,* 1009-1014.

Earlougher, R.C., Jr. 1977: *Advances in well test analysis*. SPE, New York, Dallas.

EDC, 2009: *Proposal for phase 2 MT measurement in NW-Sabalan geothermal project.* SUNA and Energy Development Corporation, report, 5 pp.

Freeze, R.A. and Cherry, J.A. 1979: *Environmental science division.* Argonne National Laboratory, EVS, web page: http://web.ead .anl.gov/resrad/datacoll/porosity.

Grant, M.A., Donaldson, I.G., and Bixley, P.F., 1982: *Geothermal reservoir engineering*. Academic Press Ltd., New York, 369 pp.

Hjartarson, Á., Lacasse, C.M., Thorgilsson, G., Ármannsson, H., Tulinius, H., Björnsson, H., Karlsdóttir, R. and Kjaran, S.P., 2008: *Puga geothermal area NW-Himalaya, India. Literature evaluation.* ÍSOR – Iceland GeoSurvey, report 2008/023, 39 pp.

Horne, R.N, 1995: *Modern well test analysis – a computer-aided approach* (2nd ed). Petroway, Inc. Palo Alto, CA, 257 pp.

James, R. 1970: *Factors controlling borehole performance*. Geothermics, 2-2, 1502–1515.

Júlíusson, E., Grétarsson, G., Jónsson, P., 2007: *Well Tester 1.0b.* User´s guide. ÍSOR – Iceland GeoSurvey, report 2008/063, 26 pp.

Karlsdóttir, R., 1997: *TEM resistivity survey on the outer Reykjanes Peninsula*. Orkustofnun, Reykjvík, report OS-9700 (in Icelandic), 63 pp.

Muffler, L.P.J. (editor), 1979: *Assessment of geothermal resources of the United States - 1978.* USGS Circular 790, Arlington, VA.

O'Sullivan, M.J., Pruess, K., Bodvarsson, G.S., and Lippmann, M.J., 2001: State of the art of geothermal reservoir simulation. *Geothermics, 30-4*, 395–429.

Sigurdsson, Ó., Bodvarsson, G.S., and Stefánsson, V., 1983: Non-isothermal injectivity index can infer well productivity and reservoir transmissivity. *Proceedings 9th Workshop on Geothermal Reservoir Engineering, Stanford University, Stanford, 479 pp*.

SKM, 2005: *NW-Sabalan geothermal feasibility study*. SUNA and Sinclair Knight Merz, final report, 140 pp.

Stefánsson, V., and Steingrímsson, B.S., 1990: *Geothermal logging I, an introduction to techniques and interpretation* (3rd edition). Orkustofnun, Reykjavík, report OS-80017/JHD-09, 117 pp.

Talebi, B., Khosrawi, K., and Ussher, G., 2005: Review of resistivity survey from the NW Sabalan geothermal field, Iran**.** *Proceedings of the World Geothermal Congress 2005***,** *Antalya, Turkey,* CD*,* 7 pp.

Tomasson, J., 1971: *Analysis of drill cuttings from Reykjanes*. Orkustofnun, Reykjavík. report (in Icelandic), 91 pp.

Wilcox, G. (editor), 2006: *The future of geothermal energy, impact of enhanced geothermal systems [EGS] on the United States in the 21. century*. Massachusetts Institute of Technology, 372 pp.

Yousefi-Sahzabi, H., 2004: Application of GIS in environmental impact assessment of Sabalan geothermal field, NW-Iran. Report 19 in: *Geothermal training in Iceland 2004*. UNU-GTP, Iceland, 439-474.

APPENDIX I: Downhole Surveys for NW-Sabalan wells

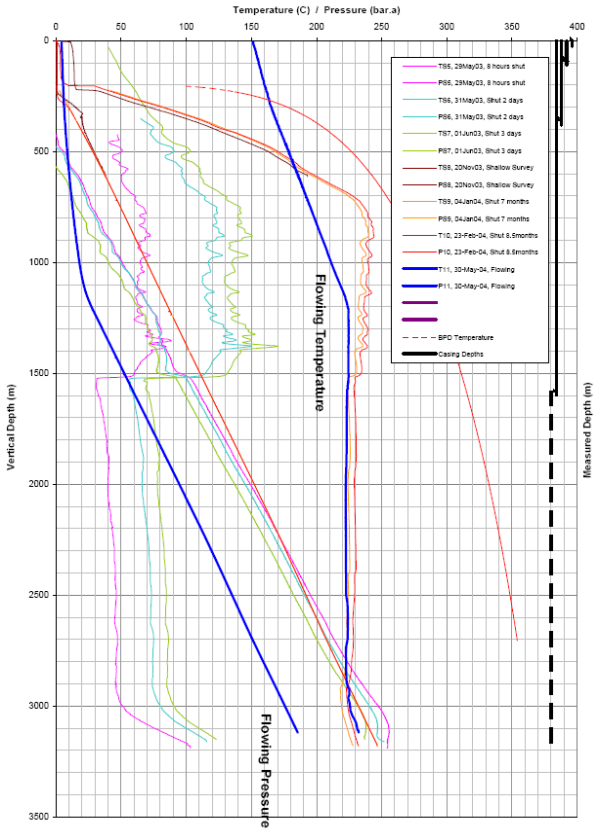

FIGURE 1: Downhole survey plot for well NWS-1 up to discharge

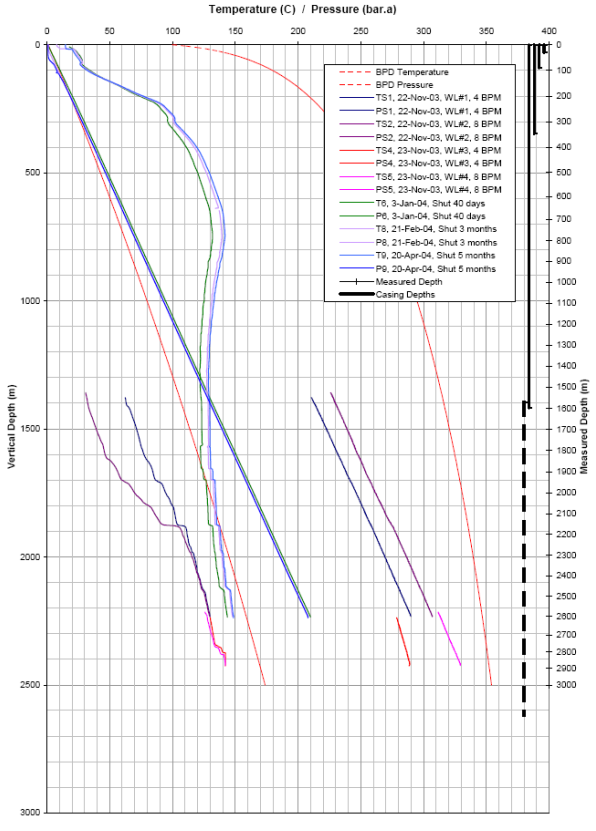

FIGURE 2: Downhole survey plot for well NWS-3

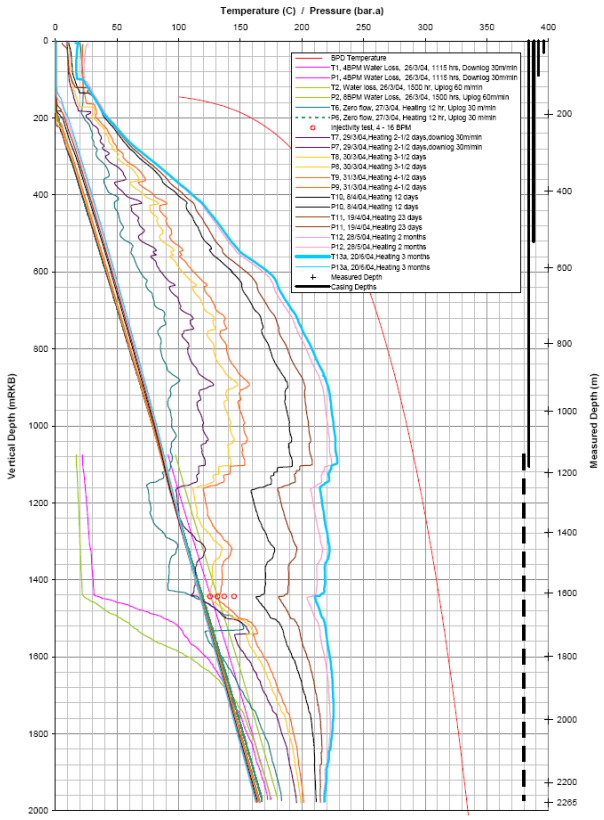

FIGURE 3: Downhole survey plot for well NWS-4

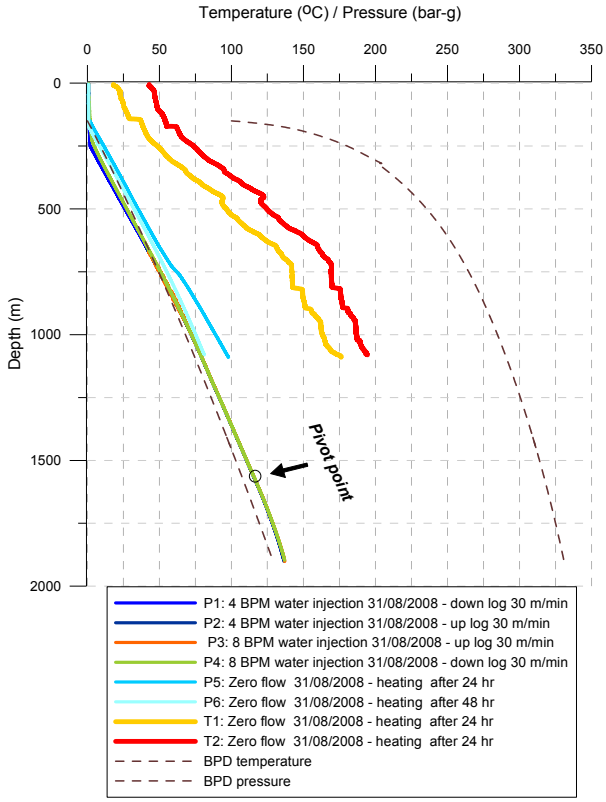

FIGURE 4: Downhole survey plot for well NWS-5D

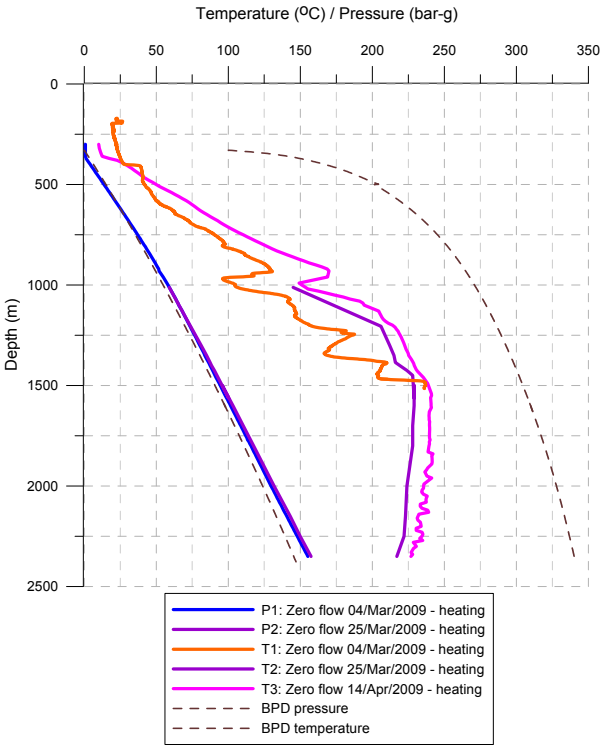

FIGURE 5: Downhole survey plot for well NWS-6D

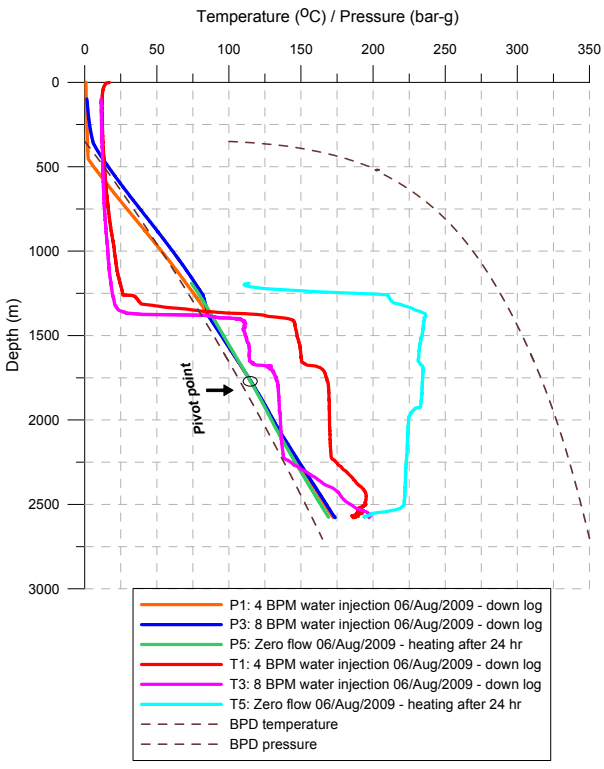

FIGURE 6: Downhole survey plot for well NWS-7D